








# Comprehensive geomechanical assessment of pillar and roof stability during secondary extraction by the room-and-pillar method

Bagdagul Uakhitova<sup>1</sup> , Bayan Almatova<sup>1\*</sup> , Akzharkyn Balgynova<sup>1</sup> ,  
Zhadrha Shilmagambetova<sup>1</sup> , Ibatolla Arystan<sup>2\*</sup> , Aruzhan Kurantayeva<sup>1</sup> ,  
Aigerim Karabatyrova<sup>2</sup> 

<sup>1</sup> K. Zhubanov Aktobe Regional University, Aktobe, Kazakhstan

<sup>2</sup> Abylkas Saginov Karaganda Technical University, Karaganda, Kazakhstan

\*Corresponding author: e-mail [balmatova@zhubanov.edu.kz](mailto:balmatova@zhubanov.edu.kz), [i.arystan@ktu.edu.kz](mailto:i.arystan@ktu.edu.kz)

## Abstract

**Purpose.** This study aims to substantiate the rational parameters of the room-and-pillar mining system for the Zhaman-Aibat copper sandstone deposit (Zhomart mine), taking into account the geomechanical characteristics of the rock mass.

**Methods.** The research employed analytical calculations based on Shevyakov, Tsern, and Chernikov methods, numerical modeling using CPS 2005, Pillars 3, and Examine 2D software packages, as well as field observations and pilot-industrial testing. The stability of inter-room and barrier pillars was assessed iteratively, considering pillar shape factor, loading conditions, and long-term strength. The effectiveness of warning (yield) pillars and different rock bolts was experimentally verified.

**Findings.** The optimal system parameters were determined as follows: panel span of approximately 70 m, extraction room width of 7 m, and inter-room pillar spacing of 16×16 m with a diameter of 9 m (pillar area about 64 m<sup>2</sup>). Experimental results confirmed the necessity of leaving 18-20 m<sup>2</sup> warning pillars, functioning in an over-stressed deformation regime. The calculated width of barrier pillars was 30 m, with a stability factor of  $n \approx 2.1$ . Structural drawbacks of steel-polymer bolts with metric threads were identified, as they can trigger progressive failure; instead, using A20V rope-thread bolts is recommended. Numerical modeling demonstrated that camouflet blasting of boreholes above barrier pillars helps unload the rock mass and reduce stress concentration.

**Originality.** For the first time under the geological conditions of the Zhomart mine, a comprehensive stability assessment of inter-room, warning, and barrier pillars was conducted using back-analysis data and in-situ observations. A quantitative relationship was established for the parameters of warning pillars operating under over-stressed deformation, substantiating the necessity of their application. The effectiveness of camouflet blasting for controlled caving of the overlying strata was also demonstrated.

**Practical implications.** The developed recommendations allow for the reduction of ore losses in pillars, the improvement of the overall stability of the mining system, and the minimization of geotechnical risks. The obtained results can be applied in designing and operating mines with similar geological and structural conditions.

**Keywords:** Zhaman-Aibat deposit, Zhomart mine, room-and-pillar mining, inter-room pillars, barrier pillars, rock bolt support, rock mass stability

## 1. Introduction

The development of copper sandstone deposits in Kazakhstan holds strategic importance, as these deposits form the core mineral resource base for the country's copper industry [1], [2]. Current trends in Kazakhstan's mining sector are focused not only on increasing production but also on the adoption of energy-efficient and environmentally sustainable technologies. Particular emphasis is placed on waste utilization, emission reduction, and improving material and technology safety standards [3]-[6]. However, operational experience at the Zhezkazgan deposit has demonstrated that applying the room-and-pillar system is associated with significant ore losses in pillars and considerable risk of roof collapse [7]-[10]. In this context, a pressing scientific and prac-

tical task is the adaptation of room-and-pillar design parameters to the conditions of specific deposits, considering their geological, structural, and geomechanical characteristics.

Digital technologies and intelligent management methods, including process modeling, automation, and machine learning, have been actively introduced into mine design and operation in recent years. These approaches make it possible to optimize equipment operating modes and enhance the accuracy of rock mass condition forecasting [11]-[16]. In addition, socio-economic and interdisciplinary factors must be considered. Several research highlights the importance of integrating the principles of the "green economy", assessing health risks to local populations in industrial regions, and fostering the development of new mining-related directions [17]-[21].

Received: 4 March 2025. Accepted: 18 September 2025. Available online: 30 September 2025

© 2025. B. Uakhitova et al.

Mining of Mineral Deposits. ISSN 2415-3443 (Online) | ISSN 2415-3435 (Print)

This is an Open Access article distributed under the terms of the Creative Commons Attribution License (<http://creativecommons.org/licenses/by/4.0/>), which permits unrestricted reuse, distribution, and reproduction in any medium, provided the original work is properly cited.

The Zhaman-Aibat copper sandstone deposit is located in the Zhanaarka district of the Karaganda region, approximately 130 km southeast of Zhezkazgan. Structurally, it is associated with the eastern limb of the Zhezkazgan-Sarysu depression and is localized within the Zhaman-Aibat horst-anticline. Based on geological and structural features, the deposit is subdivided into four sections: Central, Eastern, Western, and Northern [22].

Mineralization is primarily associated with lenticular bodies of terrigenous gray-colored rocks in the Taskuduk and Zhezkazgan formations. The ore field extends up to 14 km along strike (west–east) and about 5 km across strike. The depth of ore body occurrence ranges between 360 and 730 m, increasing toward the west and north. The morphology of the ore bodies is predominantly tabular. A total of 26 economic ore bodies have been delineated, generally of gentle dip, with thicknesses ranging from 0.5 to 18 m (average 4.33 m). The average copper grade is 1.69%, varying from 0.4 to 21.4%.

It should be noted that Kazakhstan's mineral resource base is characterized by a high diversity of ore formations, including rare-metal deposits, nickel-bearing weathering crusts, and specific mineralization environments in the lakes of Eastern Kazakhstan [23]–[27].

Regarding geological complexity, the Central and Eastern sections fall into the second complexity category, while the Western and Northern sections belong to the third. The mineral composition of the ores is dominated by chalcocite, bornite, and chalcopyrite; in polymetallic ores, galena and sphalerite also occur.

Based on a combination of geological-structural, engineering-geological, hydrogeological, and technological features, the Zhaman-Aibat deposit is regarded as an analogue of the Zhezkazgan deposit, which has been mined for decades using the room-and-pillar method. The cut-off conditions for resource estimation were approved by the State Reserves Committee of the Republic of Kazakhstan (Protocol No. 51-k of 27 January 1997).

For the Zhaman-Aibat deposit, cut-off parameters regulating the conditions for industrial-scale ore extraction were formally established. These parameters consider the specifics of copper and polymetallic ores and provide guidelines for economic (balance) and sub-economic (off-balance) categories.

For copper ores, the cut-off grade for copper content in a sample is set at 0.40%, while the minimum copper grade in boundary workings must be at least 0.80%. The combined cut-off grade for lead and zinc is set at 1.30% for polymetallic ores, with a minimum copper content of 0.30%. The minimum equivalent copper content in boundary workings is taken as 0.90%. To convert to equivalent copper, the following coefficients are applied: copper – 1.00; lead – 0.13; zinc – 0.24. Lead grades below 0.25% and zinc grades below 0.30% are excluded from calculations.

The minimum mineable thickness of ore bodies is set at 3.0 m; for thinner ore bodies, an adjustment factor (2.40%) is applied. The maximum allowable thickness of barren interlayers and sub-economic ore within ore bodies must not exceed 4.0 m. For all ore types, by-product reserves of silver, rhenium, and sulfide sulfur are additionally estimated.

Further research in the field of metallurgical and construction materials also remains relevant, including studies of the thermodynamic principles of electric smelting of concentrates, the influence of flux additives, and the modification of

cement and concrete mixes to improve their strength and durability [28]–[31].

The off-balance ore category includes ores with sub-economic grades of valuable components. The cut-off grade in a sample is set at 0.30% for copper ores, while for lead-zinc ores, it is set at 1.10% for the combined lead and zinc content. Another important indicator is the bulk density of ores: for ores with a total metal content (copper, lead, and zinc) of up to 1%, it is taken as 2.6 t/m<sup>3</sup>.

The reserves of copper ores, copper, and associated components at the Zhaman-Aibat deposit were approved by the State Reserves Committee of the Republic of Kazakhstan as of January 1, 1999 (Protocol No. 58-00-U of 16 September 2000). According to categories C1 + C2, the deposit contains 169.46 Mt of ore with an average copper grade of 1.69% and a total metal content of 2.86 Mt.

The reserve estimation was performed using the geological block method and was carried out only for a single ore type classified as “copper ores.” At the same time, drill holes, particularly in the Western section, revealed ore intervals with economic lead and zinc contents. However, it was impossible to delineate independent geological blocks of polymetallic ores during reserve estimation. As a result, the State Reserves Committee disapproved separate categories for polymetallic or lead-zinc ores. Nevertheless, the lead and zinc contents in drill holes that reached economic thresholds were calculated and officially approved.

Thus, although all reserves of the deposit were officially approved under the category of “copper ore,” the copper balance sheet also includes approved reserves of lead and zinc, which is significant for the comprehensive evaluation of the mineral resource base.

The stability of inter-room and barrier pillars in room-and-pillar mining systems has been a central problem in geomechanics for decades [32]. Despite extensive operational experience in the Zhezkazgan ore district, attempts to extrapolate its results to geologically similar deposits have demonstrated limited applicability, highlighting the necessity for new research that accounts for local geomechanical features [33], [34].

Several studies have examined the limiting spans of mined-out panels and the conditions governing their stability. For example, [35] showed that the safe panel size depends not only on the strength characteristics of the rock mass but also on tectonic stresses acting in flexure zones. Similar conclusions were confirmed by studies on roof stability in room-and-pillar mining at the Zhezkazgan ore field, where reducing the width of extraction rooms decreased the extent of roof collapses and other deposits abroad [36]–[38].

Particular attention has been given to the long-term strength of pillars. Yu et al. proposed incorporating the time-dependent degradation of rock mass strength into design criteria and outlined requirements for safety margins based on long-term stability [39]. Nazarov et al. demonstrated that the long-term safety factor should exceed the instantaneous one by at least 15%, otherwise pillars progressively lose stability under sustained loading [40]. Contemporary research also emphasizes the role of brittleness. Walton et al. suggested using uniaxial compressive strength (UCS) as a proxy indicator for brittleness, refining empirical pillar strength formulas accordingly [41].

Numerical methods are gaining increasingly widespread application. Moffat et al. proposed a “brickwork” model to evaluate pillar load-bearing capacity [42], while Toderas et al. analyzed the influence of secondary stresses arising from the interaction between adjacent rooms [43]. Liu et al. investigated the stability of old mined-out spaces during secondary extraction [44]. In contrast, Guo et al. studied the factors driving the failure of walls between pillars in deep-level mines [45].

A promising research direction is the application of machine learning methods. Li et al. demonstrated that logistic model trees can accurately classify pillar conditions based on their geometry, depth, and rock strength [46].

Considerable attention has also been devoted to roof support. Alejano et al. showed the effectiveness of cable bolts in improving pillar stability [47]. Under Kazakhstani conditions, Demin et al. substantiated the feasibility of combined bolt systems that accommodate rock layering [48]. The studies by Arystan et al. [49], [50] and Sultanov et al. [51] further confirm the necessity of selecting appropriate design parameters for support systems and employing modified materials to enhance the reliability of underground structures.

Field observations at the Zhomart mine conducted by Istekova et al. revealed that collapse zones form significantly faster than at the Zhezkazgan deposit [52], necessitating reinforced roof support measures and adjustments to room-and-pillar system parameters. Recent studies on integrated geomechanical monitoring of deposits in Kazakhstan also emphasize the relevance of modern support technologies and rock mass monitoring [53].

Additional research on salt and ore deposits demonstrates the universal nature of pillar stability problems. For example, Majeed et al. assessed pillar stability using the flat jack method in salt mine conditions. At the same time, Aitaliyev investigated the formation of arch-shaped vaults under room-and-pillar mining, which is also relevant for the Zhaman-Aibat conditions [54], [55].

Thus, the review of recent publications highlights several unresolved issues: the need to refine the parameters of the room-and-pillar system for the Zhomart mine, the experimental justification of warning pillar dimensions, and the development of practical solutions for roof bolting.

## 2. Engineering background

Ore body 4-1 of the copper sandstones is confined to the Central section of the deposit and occurs at depths ranging from -120 m (near Ventilation Shaft No. 2) to -270 m (near Ventilation Shaft No. 1). With an average surface elevation of +360 m, the depth of the ore body varies as follows: around Ventilation Shaft No. 2 it reaches 480 m, in the central part about 550 m, and in the area of Ventilation Shaft No. 1 approximately 630 m. A difference in elevation of 150 m over a distance of 5.6 km corresponds to an average dip angle of about  $1.5^\circ$  to the southwest (azimuth  $250^\circ$ ). This angle is so slight that ore body 4-1 can be considered practically horizontal for engineering calculations.

The average bulk density of the overlying strata, according to A.B. Baibatchaev, is  $\gamma = 2.7 \text{ t/m}^3$ . The ore body thickness varies from 0.5 to 13.2 m, with an average of about 4 m. Copper content ranges between 0.51 and 7.36%, averaging 1.77%. The main ore mineral is chalcocite, with bornite and chalcopyrite occurring less frequently. The Protodyakonov

strength coefficient of the ore varies from 6.1 to 13.3, with an average  $f = 9$ , which indicates moderate rock mass strength.

The natural stress state of the rock mass was evaluated from the analysis of control borehole cores using the discing method. The maximum stresses are the horizontal tectonic stresses  $\sigma_1 = \lambda_1 \cdot \gamma H$ , acting along the strike of flexural zones with an azimuth of  $70\text{--}250^\circ$ . The coefficient  $\lambda_1$  varies between 1.7 and 3.7, with an average of about 2.0. Intermediate horizontal stresses are  $\sigma_2 = \lambda_2 \cdot \gamma H$ , with  $\lambda_2 \approx 1.2$ , oriented perpendicular to the flexural zones. The minimum stresses in the system are vertical  $\sigma_3 = \gamma H$ , determined by the weight of the overlying strata. The overall scheme of principal stress distribution is presented in Figure 1.

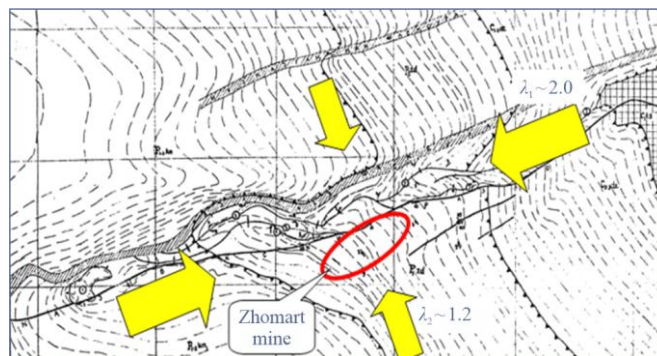


Figure 1. Conceptual representation of the natural stress state of the rock mass at the Zhomart mine based on core discing data from control boreholes

An important geomechanical parameter in pillar stability calculations is the ratio of the deformation modulus of the ore ( $E_o$ ) to that of the host rocks ( $E_r$ ). Figure 2 presents histograms of the elastic modulus distribution for different lithotypes within the Zhaman-Aibat deposit.

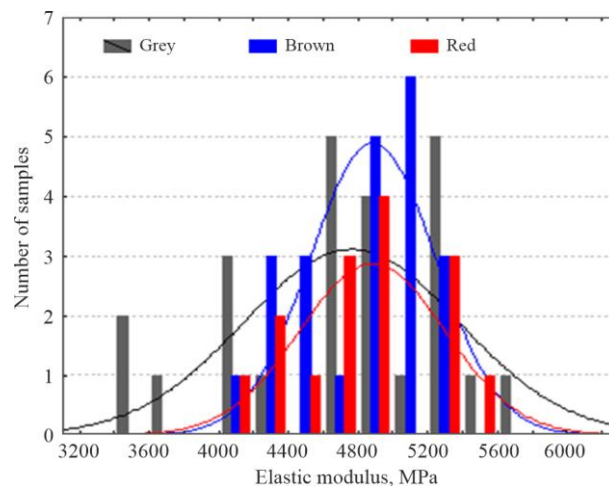
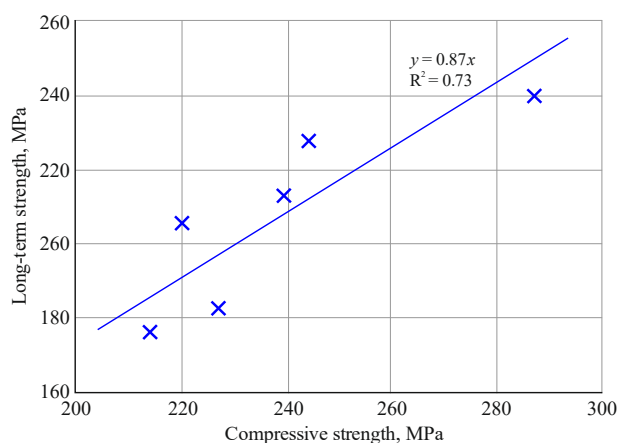


Figure 2. Distribution of elastic modulus values for various rock types at the Zhaman-Aibat deposit

Analysis of the obtained data shows that differences in elastic modulus values for gray, brown, and red sandstones fall within the range of their natural variability. In other words, no statistically significant differences between these lithotypes are observed. Therefore, in engineering calculations of inter-room pillar loading, assuming the ratio  $E_r/E_o$  equal to unity is reasonable.

Laboratory tests of samples have shown that the compressive strength of the ore-bearing sandstone across bedding is 238 MPa, while the tensile strength is 15 MPa. The ratio of tensile to compressive strength is about 6%, indicating the material's brittle nature. Under such conditions, the likelihood of pronounced rheological behavior is negligible, allowing classical strength models to predict rock mass behavior.

A critical parameter determining the rock mass's long-term stability is the ore's time-dependent (long-term) strength. According to Podzemgazprom data, the long-term compressive strength ( $\sigma_l$ ) of gray sandstones is 87% of their instantaneous strength ( $\sigma_0$ ) (Fig. 3). This ratio is of fundamental importance for evaluating the behavior of inter-room pillars. It implies that when the acting stresses do not exceed  $0.87\sigma_0$ , no new cracks form in the ore. Under such conditions, a sample or a pillar may remain stable indefinitely. However, if the applied stresses exceed the threshold of  $0.87\sigma_0$ , microcrack initiation begins in the ore mass, accompanied by acoustic emissions ("crackling"), and failure of the specimen occurs after a specific period.



**Figure 3. Relationship between instantaneous and long-term compressive strength of gray sandstones at the Zhamaan-Aibat deposit**

The ratio  $\sigma_0/\sigma_l = 1/0.87 = 1.15$  can be considered the limiting safety factor ( $n_{lim} = 1.15$ ). If the actual safety factor of an inter-room or warning pillar is less than this value, its failure becomes inevitable after a specific period of time. This safety margin corresponds to the design purpose of warning pillars, which are intended to operate in an overstressed deformation regime, where gradually increasing ground pressure leads to their crushing. Conversely, if the safety factor of a pillar exceeds the limiting value  $n_{lim} = 1.15$ , it can maintain stability for a long time, theoretically indefinitely.

Back-analysis of partial failure cases involving 49 inter-room pillars in Panels 1, 2, 3, 5, and 6 established that the ore mass strength is  $\sigma_o = 33$  MPa, with a standard deviation of 4.7 MPa and a coefficient of variation of 14% (Fig. 4). These values reflect the actual load-bearing capacity of the ore mass under operational stress conditions and confirm the necessity of selecting appropriate parameters for the room-and-pillar mining system.

Ore extraction at the Zhomart mine has been carried out since 2006 using a room-and-pillar system with columnar inter-room pillars. Initially, the system was designed with a barrier pillar spacing of 150 m and a panel span of approximately 130 m. The width of the barrier pillars was set at 20 m.

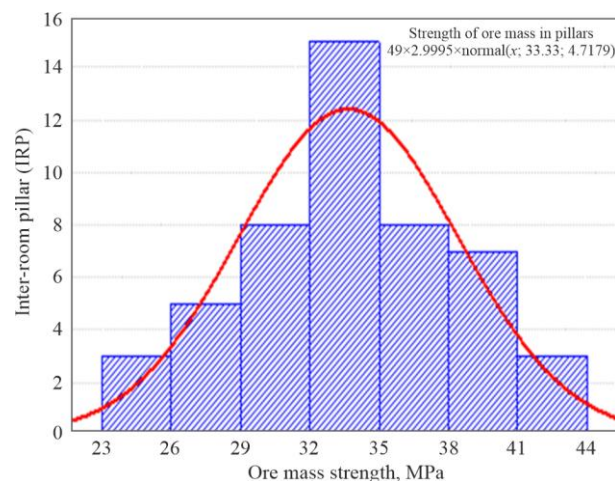


**Figure 4. Strength of the ore mass at the Zhomart mine according to back-analysis results**

In the transverse direction, each panel included eight extraction rooms and seven inter-room pillars arranged in an  $18 \times 18$  m grid. The diameter of the columnar inter-room pillars and the width of the extraction rooms were both taken as 9 m. This design solution enabled the commencement of industrial-scale ore extraction. However, during operation, manifestations of rock pressure and cases of partial pillar failure began to be recorded, necessitating additional studies of the pillars' actual strength and long-term stability.

Intensive pillar failures were observed after the development of the first three rows of inter-room pillars in Panels 1 and 2, and one row in Panel 3. This demonstrated that the initially adopted parameters of the room-and-pillar system, derived by analogy with the conditions of the Zhezkazgan mines, were unsuitable for the geological and geomechanical characteristics of the Zhomart ore mass. The subsequent analysis identified two key reasons. First, the strength of the ore mass proved to be nearly half that of the Zhezkazgan deposit. Second, the structure of the ore and host rock sequence exhibited more pronounced interbedding, including weak carbonaceous layers, significantly reducing the rock mass's overall stability.

As a result of the observed failures and the intensive destruction of columnar inter-room pillars, the parameters of the room-and-pillar system were revised. The updated design reduced the panel span to 95 m while maintaining the barrier pillar spacing of 150 m. At the same time, the width of the barrier pillars was increased to 55 m. In the transverse direction, the number of extraction rooms was reduced to six, and the number of inter-room pillars to five. A significant modification was the replacement of columnar inter-room pillars with staggered belt-type pillars, measuring  $9 \times 30$  m.

Panels 1, 2, 3, North 39, 40, and 41 were successfully mined using the adjusted parameters. Field observations showed that under these conditions, the state of the belt-type inter-room pillars and roof could be considered satisfactory.

However, despite the improved roof and inter-room pillar conditions when using the belt system, operations demonstrated that these parameters resulted in excessive ore losses within the pillars, sometimes exceeding 50%. Consequently, another revision of the design solutions was undertaken, aimed at increasing ore recovery.

In the revised system, the spacing of barrier pillars was reduced to 130 m, and the panel span was decreased to 90 m.



The width of barrier pillars was reduced to 40 m. The panel consisted of five extraction rooms and four inter-room pillars in the transverse direction. At this stage, the belt-type pillars were again replaced by columnar pillars, arranged in an 18×18 m grid. The diameter of the columnar inter-room pillars and the width of the extraction rooms were set at 9 m. This adjustment reduced ore losses and enabled a more rational use of geological space while maintaining acceptable roof and inter-room pillar stability.

Using these updated parameters, ore extraction is underway in Panels 4, 5, 6, 8, 9, 11, 12, 42, 43, 44, 49, 50, and 51. Under these geometric conditions, the overall state of the columnar inter-room pillars is assessed as satisfactory. At the same time, localized signs of pillar failure have been observed, which are accounted for in back-analyses of ore mass strength.

Steel-polymer rock bolts are used for roof support in the Zhomart mine extraction rooms. Installation is performed with a lag of about 1 m from the working face. Bolts are installed in a 1×1 m grid to a depth of 2.1 m in boreholes 35 mm in diameter. The load-bearing element is a deformed steel bar with a 22-24 mm diameter. Anchoring uses 7-8 cartridges of polymer resin per borehole. In addition, bearing plates of 130×130×6 mm with a central hole of 30 mm are applied, with fixation ensured by a nut on an M20 metric thread. The structural and geometric model of the bolt is shown in Figure 5.



**Figure 5.** Rock bolt used: 1 – deformed steel bar; 2 – threaded section, where failures are typically observed

The results of visual inspections of the extraction room roofs revealed characteristic defects in the performance of the steel-polymer rock bolt support system (Fig. 6a-c). The most frequently observed failures were bolt breakages, and their occurrence cannot be considered isolated. Less regularly, bearing plate failures were recorded, but they also represent a potential source of hazard.

Bolt failures occur predominantly along the metric thread, where the load-bearing cross-sectional area of the bar is 17-30% smaller than the deformed bar's main body. In addition, the thread acts as a pronounced stress concentrator, which accelerates the failure process (Fig. 6a). Individual cases of bearing plate detachment are associated with ruptures initiating from the central hole (Fig. 6b). The failure of even a single bolt leads to overload of adjacent bolts, triggering a chain reaction of support failure and, consequently, roof collapse of up to 3-5 m in thickness. Such cases are confirmed by numerous observed roof delaminations (Fig. 6c). In delamination zones, broken bolts are almost always recorded, while intact elements are exposed over a length of 0.5-0.8 m.

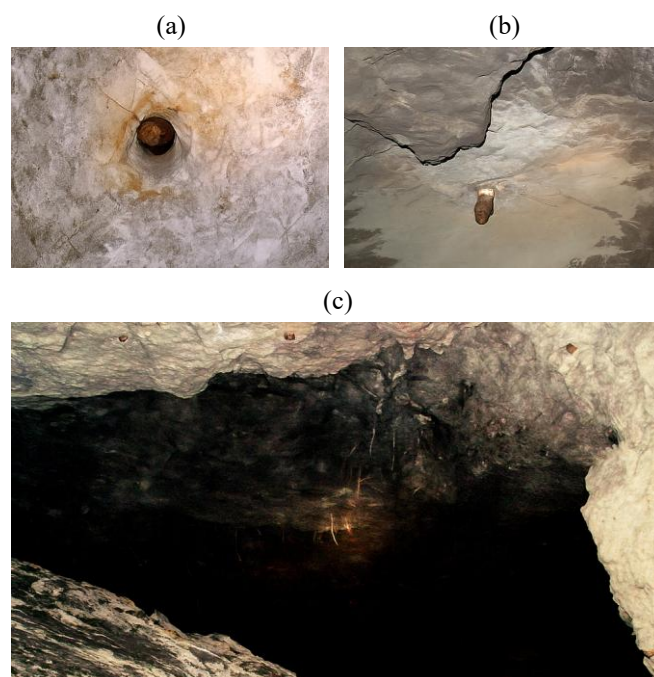


**Figure 6.** Typical forms of rock bolt failure at the Zhomart mine: (a) bolt breakage along the threaded section (remnants of the bearing plate are visible); (b) bearing plate rupture (the nut remains intact); (c) roof fall

A characteristic indicator of instability is rows of broken bolts identified along the perimeter of large roof falls with an area of up to 400 m<sup>2</sup> and a thickness of 3-5 m.

The widespread failures of rock bolt supports indicate that the current bolt design does not correspond to the geological conditions of the Zhomart mine, where the stratification of rocks includes numerous thin, weak layers that are significantly thinner than at Zhezkazgan. Due to this thinly bedded structure, roof stability in the Zhomart stopes is lower, and the loading on the bolt support is higher. Therefore, the load-bearing capacity of the rock bolt system at the Zhomart mine should be greater than that at the Zhezkazgan mines. However, the bolt parameters are nearly identical to those applied in Zhezkazgan, even though mining at Zhomart is conducted at greater depths and in weaker ore and host rocks. As a result, even extraction rooms with reduced spans of 9 m sometimes experience roof collapses.

The observed manifestations of rock pressure provide convincing evidence that the rock bolt design currently used at the Zhomart mine has a fundamental structural flaw, which promotes bolt failure and subsequent roof collapse. Therefore, the need to change the bolt type is evident. As an alternative, using rope-thread bolts of the A20V type is recommended (Fig. 7a). This design is specified in the current "Temporary Instruction..." on rock support at the Zhaman-Aibat mine. Bolts of this type have already proven themselves in industrial practice and are used at several mines of the corporation in Eastern Kazakhstan, including the Artemyevsky, Nikolaevsky, Orlovsky, Irtyshsky, and Yubileyno-Snegirikhinsky mines (Fig. 7b). Their application increases the load-bearing capacity of the support system. It reduces the likelihood of roof falls under the challenging conditions of thinly bedded rock masses.

An experimental secondary extraction of belt-type inter-room pillars was conducted to recover remaining reserves and backfill the mined-out space in Panel 2.

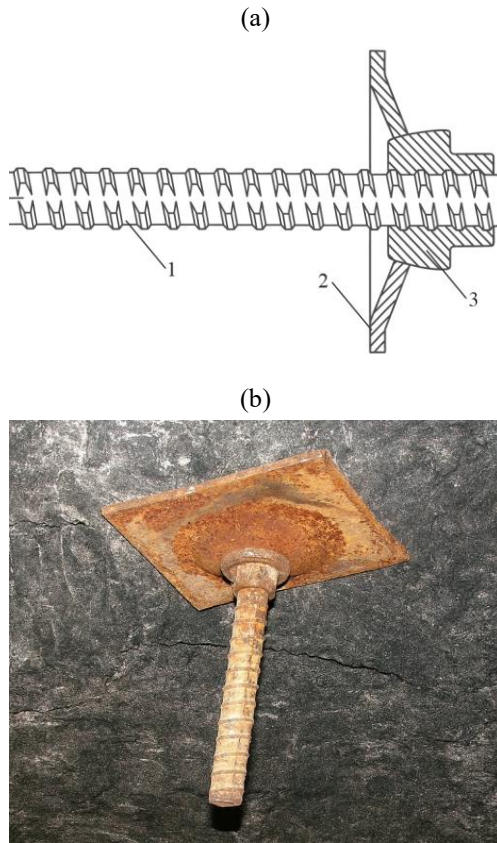


Figure 7. Rope-thread bolt design: (a) schematic illustration; (b) installed bolt in the rock mass; 1 – bolt; 2 – bearing plate; 3 – tightening nut

Based on the results of this industrial experiment, it was recommended that secondary extraction be carried out in two stages: in the first stage, the belt is cut into columnar pillars with an area of 80-90 m<sup>2</sup>, arranged on an 18×18 m grid; in the second stage, the columnar pillars are mined with the mandatory preservation of warning pillars.

During the trial, it was determined that the cross-section of a warning pillar should be approximately 20 m<sup>2</sup> (4×5 m). After blasting the inter-room pillars, stabilization accompanied by localized roof collapses occurred within 24 hours, meaning that the minimum required waiting time at the stope should not be less than one day. The limiting span at which spontaneous caving of the overlying strata occurred was 45 m. The collapse, covering an area of about 5000 m<sup>2</sup>, did not generate a significant air blast, as it took place over a rock mass that had previously undergone partial collapse during localized deformation.

At the same time, the trial revealed cases of roof collapse onto blasted ore in the loading zone. Typically, this was associated with discontinuities in the roof integrity within working areas between pillars adjacent to the mined-out inter-room pillars. The discontinuity formed after roof sagging, detachment of bearing washers, and bolt failures in the threaded section. Vertical cracks propagating along the rooms were also observed. In such situations, forced removal of delaminated rock and re-bolting the roof with steel-polymer bolts was carried out. It should be emphasized that the problem of immediate roof support in extraction rooms using rock bolts identified during the initial development of the room-and-pillar system was even more acute during secondary extraction. This was caused by the exposed roof's increased spans and the supporting pillars' reduced stiffness.

Two approaches were considered to ensure roof stability and increase ore recovery from inter-room pillars (Fig. 8).

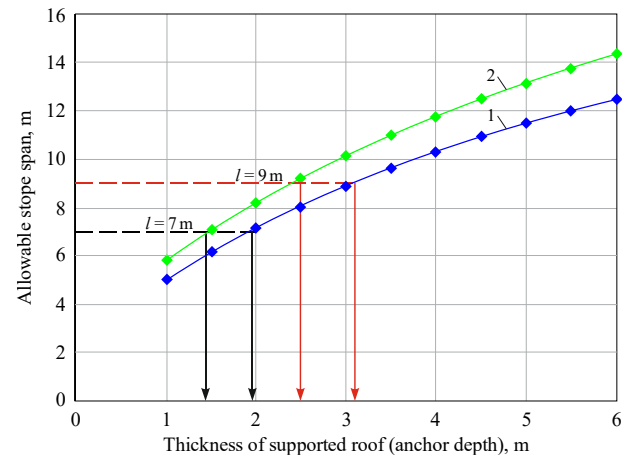


Figure 8. Determination of the required bolt length for extraction room spans of 9 and 7 m at roof rock tensile strengths of: 1 – 1.5 MPa; 2 – 2.0 MPa

The first approach involves reinforcing roof support by modifying the bolt design and increasing the installation depth to 3 m. The second option entails reducing the extraction room width to 7 m while maintaining the bolt installation depth at 2.1 m, but with the mandatory replacement of the current bolt type with a stronger alternative.

The first option requires purchasing new booms for Ro-bolt installations with a minimum length of 3.2 m. It is associated with increased steel and polymer resin consumption, resulting in higher roof support costs. The second option reduces recoverable ore reserves, complicates the operation of large-scale equipment, and reduces its overall efficiency. Based on the analysis, the management of Kazakhmys Corporation decided to test a modified room-and-pillar mining system with extraction room spans reduced to 7 m.

### 3. Research methodology

#### 3.1. Principles of inter-room pillar (IRP) strength calculation

The fundamental principles of pillar stability assessment were formulated as early as the 1940s by Academician L.D. Shevyakov. In the most general form, the stability condition can be expressed as:

$$nK_l\gamma HS \leq F\sigma_p, \quad (1)$$

where:

$n$  – factor of safety;

$K_l$  – loading coefficient;

$S$  – roof area supported by a single pillar with area  $F$ ;

$\sigma_p$  – pillar strength is considered based on the shape factor.

The left-hand side of the expression represents the load on the pillar, multiplied by the safety factor  $n$ , while the right-hand side corresponds to its load-bearing capacity.

In the case of columnar inter-room pillars arranged in a square grid, the roof area supported by a single pillar ( $S$ ) is defined as:

$$S = (l + d)^2, \quad (2)$$

where:

$l$  – width of the extraction room (clear span);

$d$  – pillar diameter.

Thus, the sum  $(l + d) = a$  defines the pillar spacing (grid dimension).

To determine the optimal pillar diameter and grid parameters for a given chamber span, the following relationship is used:

$$\frac{S}{F} \leq \frac{\sigma_p}{nK_l\gamma H}. \quad (3)$$

The main task in the practical application of this approach is to determine the values of the loading coefficient  $K_l$  and the pillar strength  $\sigma_p$ .

Based on an extensive series of numerical simulations (approximately 4.5 thousand panels and 560 thousand inter-room pillars), considering the statistical variability of parameters, D.V. Moskvina established a relationship for the average loading coefficient of pillars within a panel. In analytical form, it can be expressed as:

$$K_l = 0.5 \ln \frac{L_e F}{h \left( \frac{E_r}{E_0} \cdot \frac{d}{h} + 1 \right)} - 2.5, \quad (4)$$

where:

$L_e$  – equivalent span of the mined-out panel space;  
 $d, h$  – diameter and height of the inter-room pillar (IRP);  
 $E_r/E_0$  – ratio of the host rocks and ore deformation moduli.

The obtained relationship makes it possible to account not only for the geometric parameters of the room-and-pillar system, but also for differences in the elastic properties of the ore mass and the host rocks. Figure 9 shows the approximation of experimental data, demonstrating good agreement of the analytical model with the results of numerical simulations. The strength of an inter-room pillar  $\sigma_p$  is determined from the ore mass strength  $\sigma_o$ , considering the shape factor  $K_f$ .

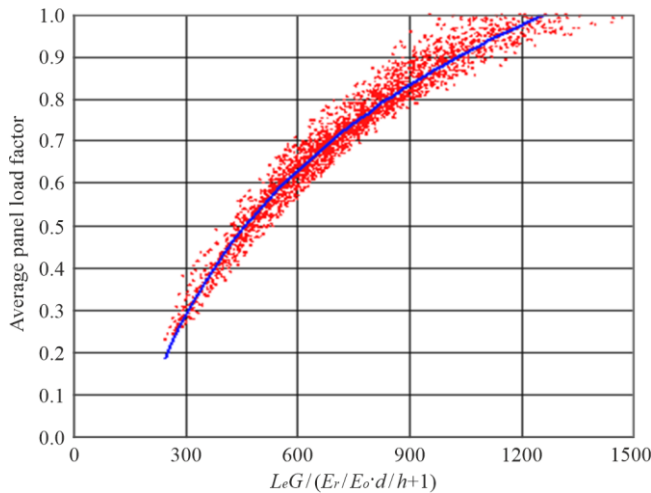


Figure 9. Dependence of the loading coefficient on the combined parameters of the mined-out space and supporting pillars

Numerous expressions for determining the pillar shape factor as a function of the ratio  $d/h$  are reported in the literature. In the “Temporary Instruction on Pillar Design...” (IGD named after D.A. Kunaev), the shape factor is  $K_f = d/h$ . As shown in Figure 10, this dependence is excessively steep: it significantly underestimates the strength of slender pillars ( $d/h < 1$ ) and, conversely, overestimates the strength of squat pillars  $d/h > 1$ .

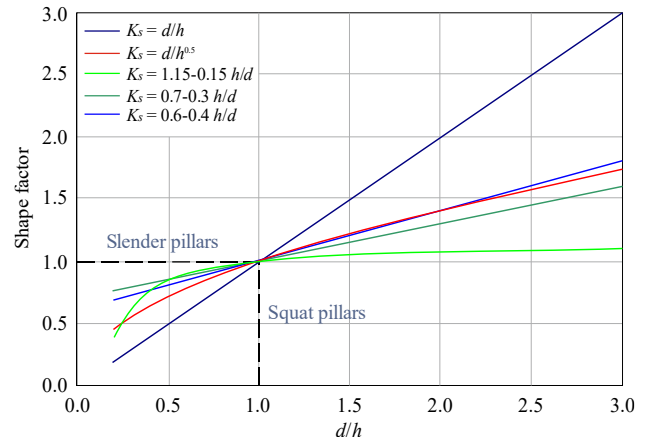


Figure 10. Determination of the pillar shape factor

According to back-analysis of pillar strength performed by specialists from RGGU and GGU ZhCM, under the conditions of the Zhezkazgan deposit, the shape factor dependence is most accurately described by the Tsern formula:

$$K_f = \sqrt{\frac{d}{h}}. \quad (5)$$

It should be emphasized that this formula forms the basis of the “Methodology for Assessing the Stability of Pillars Involved in Secondary Mining”, which confirms its practical significance and high reliability for design calculations.

### 3.2. Calculation of inter-room pillars (IRPs) for the Zhomart mine conditions

Equations (1)-(4), presented earlier, do not allow a direct analytical determination of the required pillar size, since the pillar cross-sectional area  $F$  appears simultaneously in both the left- and right-hand sides of Equation (3). Therefore, the needed pillar dimensions were determined using a step-by-step iterative method, progressively refining the parameters until Condition (3) was satisfied.

As a result of these iterative calculations, it was established that Condition (3) is satisfied with a safety factor  $n = 1.97$  (practically equal to 2) when the following room-and-pillar system parameters are adopted. The mining depth is 550 m, and the panel span is 71 m. Across the panel width, five extraction rooms of 7 m each and four inter-room pillars are provided. The pillar diameter is 9 m, corresponding to a cross-sectional area of 64 m<sup>2</sup>. Thus, the pillar grid spacing is 16×16 m (the sum of the room width and the pillar diameter). The mining height of the ore body is determined by the dimensions of the equipment in use and is set at 7 m.

With these system parameters, the loading coefficient for the set of inter-room pillars, calculated using Equation (4), was  $K_l = 0.32$ . The maximum possible value of the support pressure concentration factor ( $K_c^{\max}$ ), arising on the edge pillars during secondary panel extraction, was determined using the formula of D.V. Mosyakin:

$$K_c^{\max} = 0.37 \cdot l_n \cdot K_l + 1.8. \quad (6)$$

At an average loading coefficient of  $K_l = 0.32$ , the value was calculated as 1.4. This indicates that during secondary extraction, the average safety factor, initially equal to  $n = 2$ , decreases to 1.4. Consequently, the above parameters of the room-and-pillar mining system can be considered acceptable for the geomechanical conditions of the Zhomart mine.



A verification calculation of inter-room pillar stability was performed using the CPS 2005 software package (RGGRU). At a mining depth of 550 m, a panel with a mining height of 7 m and a total area of  $71 \times 320 \text{ m} = 22720 \text{ m}^2$  was simulated. The panel was supported by 80 pillars (four rows of 20 pillars each). Each pillar had an area of  $64 \text{ m}^2$  (diameter 9 m) and was arranged on a  $16 \times 16 \text{ m}$  grid. The perimeter of the modeled panel was 782 m.

The numerical modeling results showed that the overall loading coefficient for the set of inter-room pillars, at an equivalent span of the mined-out space  $L_e = 69 \text{ m}$ , was  $K_l = 0.35$ . At the same time, the loading and stability of pillars within the panel were found to be significantly non-uniform (Fig. 11).

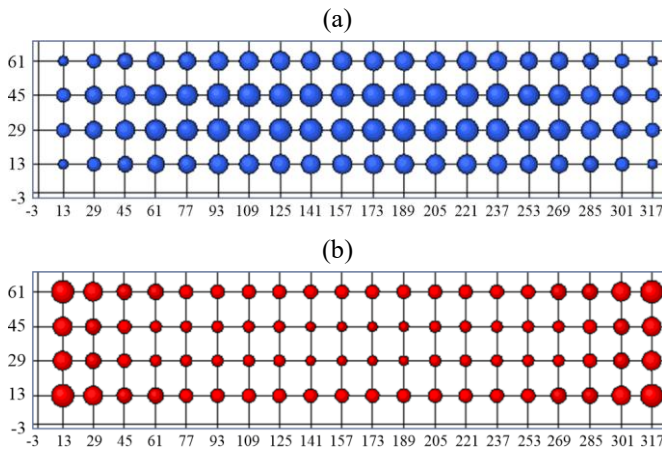


Figure 11. Non-uniformity of (a) loading and (b) safety factor of inter-room pillars in the panel (circle diameters are proportional to the loading coefficient and safety factor of each pillar)

The central rows of inter-room pillars bear the most significant load, resulting in their minimum safety factor. Conversely, the edge pillars are less loaded, while the highest stability is characteristic of the corner pillars (Fig. 12).

The average safety factor of the panel's entire set of inter-room pillars is  $n = 1.92$ , with a standard deviation  $S_d = 0.38$ . The coefficient of variation,  $V = S_d / n = 0.20$ , indicates an acceptable level of parameter variability. According to Popov's formula (7), the reliability of the inter-room pillar system under these conditions is 85%, meaning that the probability of failure of the entire pillar system does not exceed 15%:

$$P = 1 - \frac{(nV)^2}{[(nV)^2 + (n-1)^2]} \quad (7)$$

The results of the obtained verification stability calculation can be considered satisfactory. Additionally, pillar stability during secondary extraction was assessed using the Pillars 3 software, which simulated pillar extraction row by row across the panel width. The modeling results are shown in Figure 13.

Data analysis showed that as secondary extraction advanced toward the panel center, the concentration of support pressure gradually increased from 1.1 to 1.2. Accordingly, the safety factor of the central pillars at the boundary of the caving zone decreased: from its initial value of 1.53 after primary extraction of room reserves, it dropped to 1.29.

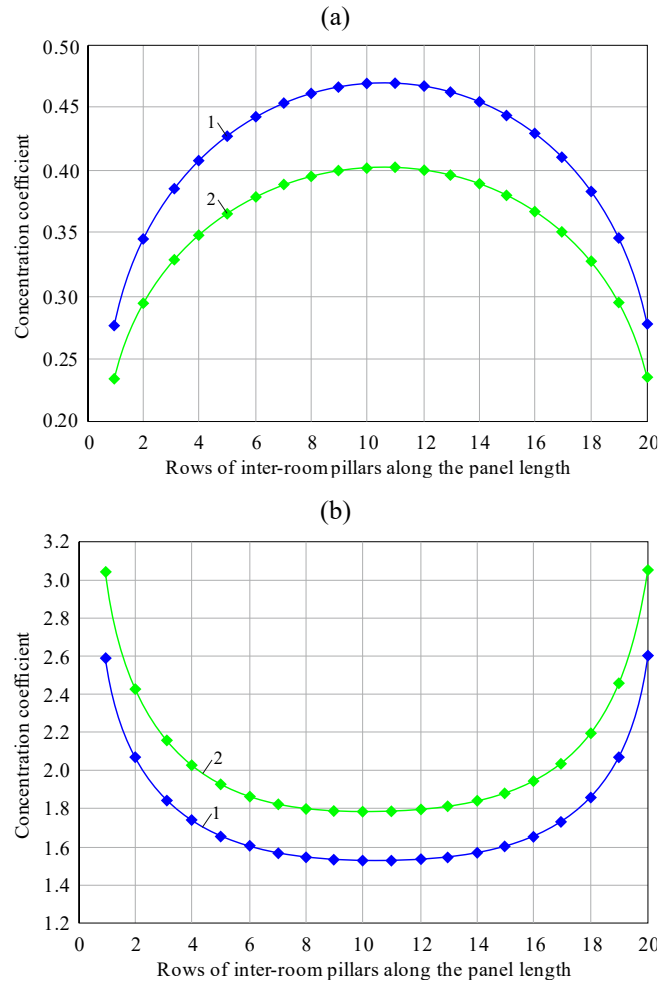


Figure 12. Loading (a) and safety factor (b) of inter-room pillars in the panel: 1 – central rows; 2 – side rows

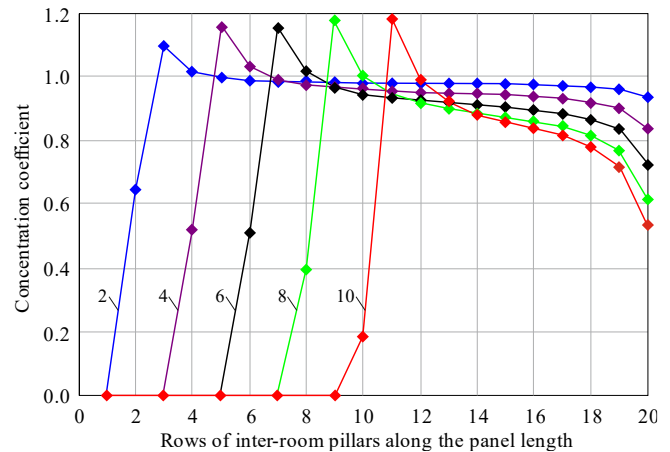


Figure 13. Concentration of support pressure on the central rows of inter-room pillars during the progression of secondary extraction: 2, 4, 6, 8, 10 – number of extracted rows

However, this value remains sufficient to allow secondary extraction from the open mined-out space without a critical loss of rock mass stability.

Thus, the verification stability analysis of inter-room pillars during secondary mining produced a positive outcome and confirmed the acceptability of the adopted room-and-pillar system parameters for the geomechanical conditions of the Zhomart mine.



### 3.3. Calculation of barrier pillars

The width of belt-type barrier pillars ( $A$ ) is determined from the condition that they must sustain the full weight of the overlying strata above the entire panel. In this case, the formula of Academician L.D. Shevyakov is applied:

$$A = \frac{L}{\frac{\sigma_p}{n\gamma H} - 1}, \quad (8)$$

where:

$L$  – span of the mined-out panel (clear width);

$\sigma_p$  – strength of the barrier pillar ( $\sigma_p = \sigma_m K_f$ );

$\sigma_m$  – strength of the ore mass;

$K_f$  – pillar shape factor.

The main uncertainty in practical calculations is associated with selecting the shape factor  $K_f$  for wide belt-type pillars. As shown in the literature data (Fig. 10), obtained from laboratory experiments at large  $A/h$  ratios (pillar width/height), considerable discrepancies are observed.

To refine the shape factor, it is advisable to use the theoretical solution proposed by A.K. Chernikov, which considers the average value of ultimate stresses for a belt-type pillar in the absence of bonding at the contacts with the host rocks:

$$\sigma_p = 2C \cdot \operatorname{ctg}^2 \left( \frac{\pi}{4} - \frac{\varphi}{2} \right) \cdot (e^a - 1) / \alpha, \quad (9)$$

where:

$C, \varphi$  – cohesion and angle of internal friction of the ore mass;

$\alpha$  – parameter accounting for friction at the contacts with friction angle  $\delta$  and for the geometry of a pillar of width  $\delta$  and height  $h$ :

$$\alpha = \operatorname{tg} \delta \cdot \operatorname{ctg}^2 \left( \frac{\pi}{4} - \frac{\varphi}{2} \right) \cdot \frac{a}{h}. \quad (10)$$

If we take into account that:

$$2C \cdot \operatorname{ctg}^2 \left( \frac{\pi}{4} - \frac{\varphi}{2} \right) = \sigma_m. \quad (11)$$

Then Equation (9) can be reduced to the form:

$$\sigma_p = \sigma_m \cdot \frac{(e^a - 1)}{\alpha}. \quad (12)$$

This means that the theoretical value of the shape factor  $K_f$  for wide squat belt-type barrier pillars is determined by the following Expression:

$$K_f = \frac{(e^a - 1)}{\alpha}. \quad (13)$$

In the case of belt-type pillars with transport crosscuts, A.K. Chernikov suggested using the Shirko-Dreyer parameter  $\mu$ , defined as:

$$\mu = \frac{2F}{U_h}, \quad (14)$$

where:

$F$  – area of the barrier pillar between crosscuts;

$U$  – perimeter of the barrier pillar between crosscuts;

$h$  – height of the barrier pillar.

Then, for the calculation of the shape factor  $K_f$ , the following formula is applied:

$$K_f = \frac{e^{\beta \cdot \mu} - 1}{\beta \cdot \mu}, \quad (15)$$

where:

$$\beta = \operatorname{tg} \delta \cdot \operatorname{ctg}^2 \left( \frac{\pi}{4} - \frac{\varphi}{2} \right). \quad (16)$$

Neither Baibatchaev A. B. (at the exploration stage of the deposit), nor the IGD named after D.A. Kunaev (K.K. Tulebaev, 2004-2005), nor LLC “Podzemgazprom” (E.S. Oksenkruhg, 2006-2007) determined the internal friction angle of the ore and rocks at the Zhomart mine. Considering that the Zhaman-Aibat deposit belongs to the same industrial type as the Zhezkazgan deposit, and given the homogeneity of the rock complexes, the internal friction angle of the rock mass ( $\varphi$ ) and the friction angle along weak contacts ( $\delta$ ) for Zhaman-Aibat can be adopted by analogy with Zhezkazgan.

At the Zhezkazgan deposit, the internal friction angle of rocks ( $\varphi$ ) was determined by VNIMI in the 1960s, based on in-situ shear tests of prismatic specimens conducted during the design and construction of KZB-3. It was found to be  $\varphi = 35^\circ$ . Under the same conditions, the friction angle along weak contacts was established as  $\delta = 12^\circ$ . This means the load-bearing capacity along weak contacts is 3.3 times lower than in the intact rock mass ( $\operatorname{tg} 35^\circ / \operatorname{tg} 12^\circ$ ). Taking into account the interbedded structure of the rocks with numerous weak carbonaceous layers at the Zhomart mine, the following parameters were adopted: no cohesion, contact friction angle  $\delta = 12^\circ$ , which corresponds to a parameter value of  $\beta = 0.77$ .

The calculations of barrier pillar parameters according to Formulas (8)-(16) were performed using an iterative method. As an initial case, the barrier pillar width was taken as  $A = 30$  m, and the distance between transport crosscuts as  $B = 45$  m. In this case, the cross-sectional area of the barrier pillar was  $F = A \cdot B$ , the perimeter  $U = 2(A + B)$ , and the Shirko-Dreyer parameter  $\mu$ , at a mining height of  $h = 7$  m, equaled 2.57 (Fig. 14).

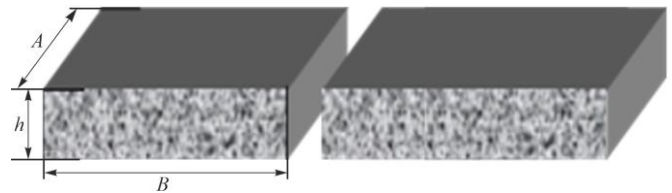


Figure 14. Scheme for barrier pillar calculation

The shape factor  $K_f$  of such a pillar, calculated using Equation (15), was 3.2. Then, with a panel span  $L = 71$  m and mining depth  $H = 550$  m, and at a safety factor  $n = 2$ , the required width of the barrier pillar according to Equation (8) was determined to be 28 m. Considering rounding, it was adopted that for a panel span  $L = 71$  m, the barrier pillar width is  $A = 30$  m. In this case, the pillar spacing grid is  $L + A = 100$  m. For verification, the average acting stresses  $\sigma_a$  in the barrier pillars were determined using the corresponding Formula  $\sigma_a = \gamma H \cdot \frac{L + A}{A}$ , which at a mining depth

of 550 m, a panel span of 71 m, and barrier pillar width of 30 m gave  $\sigma_a = 49.0$  MPa.

The ultimate stresses for the barrier pillars were calculated as 105.6 MPa. Thus, the resulting safety factor is  $n = 2.1$ . This result meets the design requirements and confirms that

the adopted system parameters are acceptable for the conditions of the Zhomart mine.

In this calculation, the safety factor of barrier pillars was set as  $n = 2$ . Compared with the values traditionally used at the Zhezkazgan deposit, where the safety factor for barrier pillars is reduced to the level accepted for inter-room pillars, the design for the Zhomart mine follows a more conservative approach.

As strength characteristics of the ore mass, the calculations employed back-analysis data derived from cases of partial failure of inter-room pillars under rock pressure. This approach is considered more reliable than conventional laboratory tests of individual samples, which generally fail to account for several weakening factors: jointing coefficients, weak interlayers, specific contact conditions, damage to the rock mass from blasting, and the long-term effects of loading. Back-analysis data makes it possible to avoid overestimated design safety factors more accurately reflect actual operating conditions. In addition, the load-bearing capacity of barrier pillars was calculated under the assumption of the least favorable contact conditions, which provides an additional margin of reliability in the conclusions.

Operational experience at the Zhezkazgan deposit, where the room-and-pillar system with deposit subdivision into extraction units (barrier pillars) has been used for more than 50 years, confirms the validity of this approach. Over this period, more than 18000 inter-room pillars have been mined, with barrier pillar failures being isolated cases. The overall share of ore losses in barrier pillars was about 40%, which is explained by their high reliability. This experience demonstrates that the safety factor of barrier pillars in design practice has traditionally been taken as overly conservative. In contrast, for the conditions of the Zhomart mine, the use of back-analysis results is a more justified and adequate approach.

## 4. Results and discussion

### 4.1. Calculation of barrier pillars

The first industrial trials of blasting columnar inter-room pillars (IRPs) were carried out in Panels 4 and 5 in February 2009. In Panel 4, during the extraction of Pillar No. 73 (February 21, 2009), a warning pillar with an area of about 8 m<sup>2</sup> (4×2 m) was left in place. Under these conditions, the stope roof maintained stability, and the blasted ore was successfully loaded. The warning pillar preserved its load-bearing capacity for several months, which can be explained by its location in the corner part of the panel.

In contrast, no warning pillar was left during the extraction of Pillar No. 73 in Panel 5 (February 24, 2009). As a result, the stope roof exhibited significant visual sagging, which made safe ore loading impossible. Within 24 hours, a roof collapse occurred, covering an area of about 400 m<sup>2</sup> with a thickness of 2.5 m.

Thus, the results of the initial trials demonstrated that under the geomechanical conditions of the Zhomart mine, secondary extraction of inter-room pillars from open mined-out space in weak, frequently interbedded roofs is possible only with the mandatory preservation of warning pillars. Consequently, optimizing the parameters of the primary extraction of room reserves and the warning pillars used during subsequent secondary extraction is necessary.

During pilot-industrial tests of secondary pillar extraction in Panel 2, warning pillars with areas ranging from 20 to

45 m<sup>2</sup> were left at different stages. The experiments established the following:

- extraction of inter-room pillars without leaving a warning pillar inevitably leads to the collapse of the immediate roof up to 5 m thick, which buries the blasted ore and makes loading impossible;
- leaving warning pillars of excessive size (over 40 m<sup>2</sup>) delays the caving of the overlying strata, necessitating their additional forced destruction by blasting, which increases operational risks;
- to temporarily support the immediate roof in the face zone with a thickness of up to 10 m, a warning pillar of optimal dimensions must operate in an overstressed deformation regime.

The behavior of a warning pillar operating in the overstressed deformation regime is illustrated by the scheme of full IRP deformation (Fig. 15).

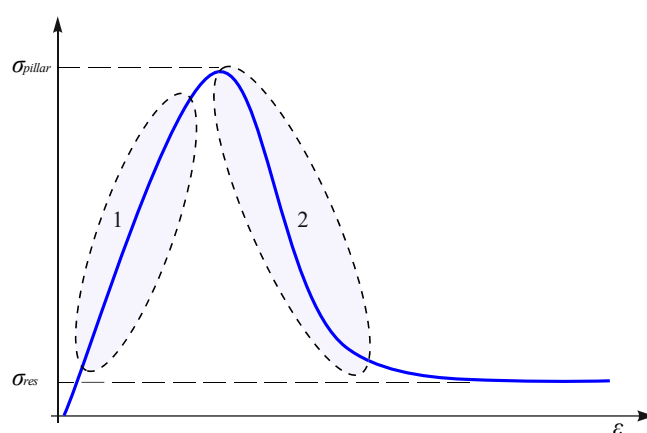


Figure 15. Scheme of full deformation of an inter-room pillar (IRP): 1 – elastic state of the pillar; 2 – overstressed state of the pillar

In the overstressed state, the pillar retains a certain load-bearing capacity  $\sigma_{pillar}$ , which decreases with progressive deformation until reaching the residual strength  $\sigma_{res}$ . This means that the safety factor of a warning pillar may be less than 1.0. The dynamics of pillar strength reduction in the overstressed state, according to M.K. Teplov for the Zhezkazgan deposit, are shown in Figure 16. The obtained dependencies indicate that when the cross-sectional area of a pillar decreases to less than 40% of its initial value,  $F$ , the residual load-bearing capacity,  $N(x)$ , is reduced to about 20% of the maximum value,  $N$ .

The warning pillar parameters for the Zhomart mine were calculated based on the requirement to support the weight of an immediate roof cantilever with a thickness (with a safety margin) of 10 m and an area of 256 m<sup>2</sup>. Under these conditions, the cantilever weight amounted to 7000 t.

A warning pillar in the overstressed deformation regime must retain sufficient residual load-bearing capacity to withstand this weight. For example, a pillar with an area of 20 m<sup>2</sup> has a residual load-bearing capacity of 8.6 thousand t, which exceeds the calculated load. For a pillar with an area of 18 m<sup>2</sup>, the residual capacity is about 7.7 thousand t, which also meets the required conditions.

Thus, warning pillars with an area of 18–20 m<sup>2</sup> are capable, in the overstressed state, of reliably supporting the immediate roof cantilever 10 m thick, without bringing the rock mass to the stage of complete strength loss.

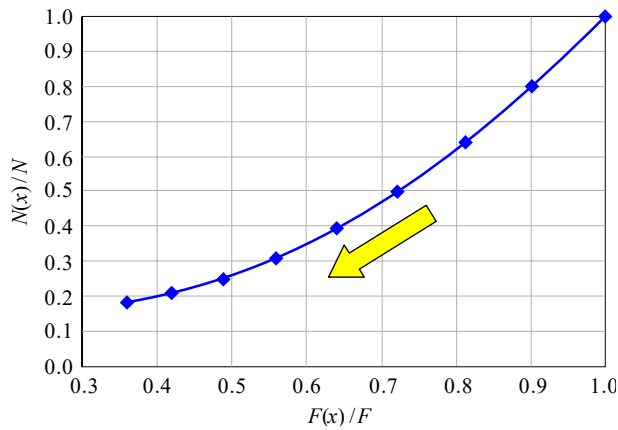


**Figure 16. Reduction in pillar load-bearing capacity in the overstressed state  $N(x)/N$  with decreasing cross-sectional area  $F(x)/F$**

It remains to be verified that the loads acting on warning pillars are sufficient to ensure their subsequent failure. Figure 17 presents the calculated values of loading coefficients and safety factors for warning pillars of different areas, obtained using the Pillars 3 software.

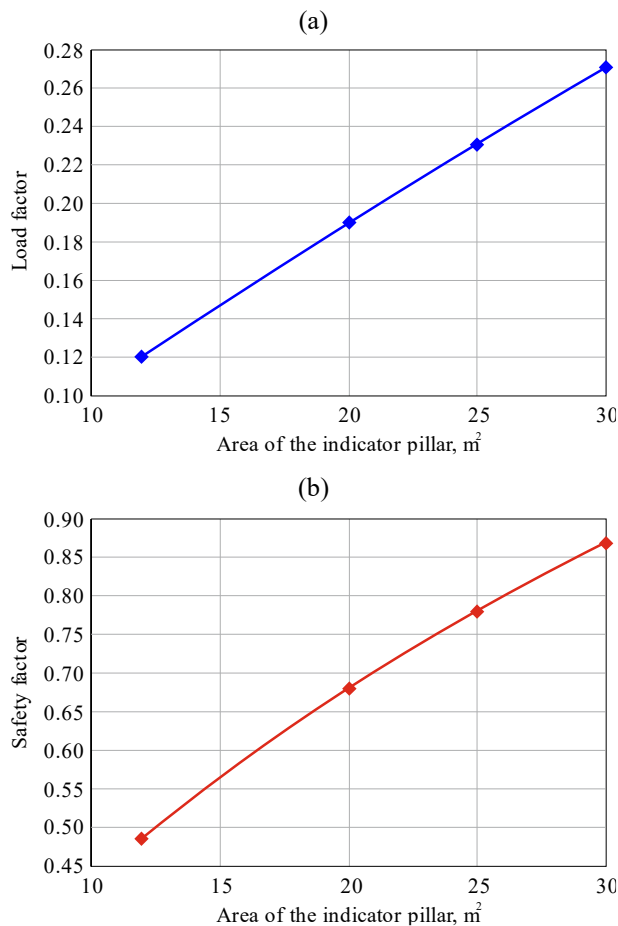


**Figure 17. Loading coefficients (a) and safety factors (b) of warning pillars in the center of the panel after half-panel extraction**

In the calculation, the worst-case scenario was simulated after half of the panel had been mined out, when the concentration of support pressure on the remaining pillars reached its maximum values. The graphs demonstrate that as the area of a warning pillar increases, the load acting on it also in-

creases. However, the ultimate load-bearing capacity grows faster, leading to a higher safety factor.

When warning pillars with an 18-20 m<sup>2</sup> area are left in place, the loading coefficient ranges between 0.18 and 0.20, while the safety factor is 0.65 and 0.68. This indicates that such pillars will gradually fail under rock pressure while temporarily supporting the immediate roof cantilever in the overstressed deformation regime. Their ultimate failure and subsequent inclusion into the caving zone should occur during the extraction of the next row of inter-room pillars, thereby ensuring controlled development of the caving process.

#### 4.2. Prediction of overburden behavior

The cumulative experience of complete subsidence of the overburden to the surface after the failure or extraction of pillars under the conditions of the Zhezkazgan deposit is presented in Figure 18. Observations show that the conditions under which all hangings are eliminated and complete overburden displacement to the surface occur are well described by a dependence with a correlation coefficient of 0.76:

$$H \leq 0.85L_e, \quad (17)$$

or, in a more general form:

$$L_e \geq 1.13H, \quad (18)$$

where:

$H$  – mining depth;

$L_e$  – critical equivalent span of underworked space.

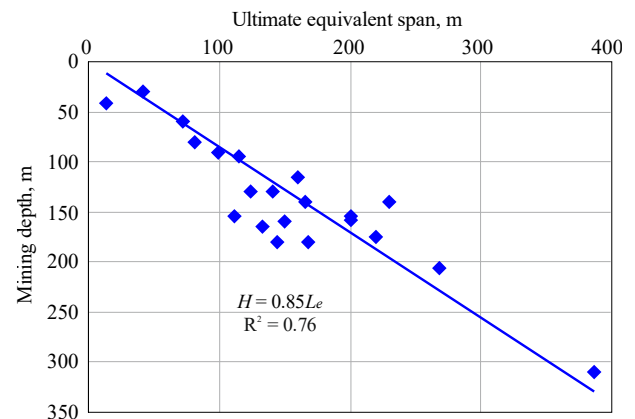


**Figure 18. Criterion for overburden subsidence to the surface at the Zhezkazgan deposit**

Comparison of these findings with the normative data presented in the “Temporary Regulations on the Protection of Structures at Deposits with an Unstudied Subsidence Process” (VNIMI, 1986) shows that the condition of overburden collapse reaching the surface during the mining of isolated medium- and the following expression describes thick-bedded deposits under caving systems:

$$H < k_1 \cdot L_e, \quad (19)$$

where:

$k_1$  – coefficient reflecting the strength factor  $f$  of the overlying strata.

The stronger the overburden mass, the lower the value of coefficient  $k_1$  (Fig. 19). For the Zhezkazgan deposit, according to Equation (17), the coefficient value is  $k_1 = 0.85$ . The Zhezkazgan data show good agreement with the general dependence if the weighted average strength coefficient of the overburden is taken as  $f = 18$ .



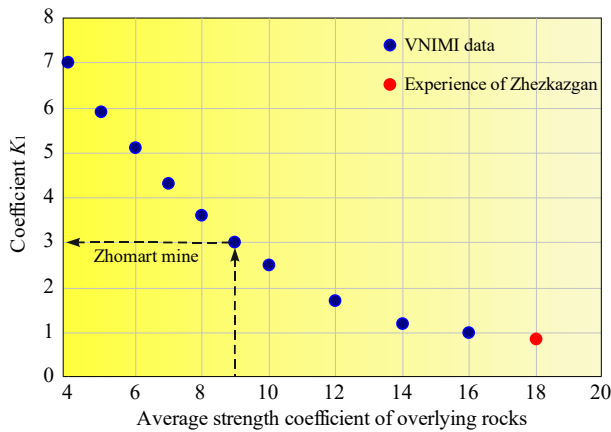


Figure 19. Values of coefficient  $k_1$  in the criterion of complete overburden subsidence to the surface as a function of the weighted average strength of overburden rock

It should be noted that this value was obtained while accounting for the lateral confinement of the rocks by high tectonic stresses.

Under the conditions of the Zhomart mine, the average rock strength is estimated at  $f=9$  (the technical project of GPI specifies  $f=8.9$ ). At the same time, the ore mass strength is about twice as low as at the Zhezkazgan deposit, and the level of horizontal tectonic stresses contributing to overburden hanging due to lateral confinement is also approximately two times lower. As a result, the calculated coefficient value is  $k_1=3$ . This means that during secondary extraction, full subsidence of the overburden to the surface, eliminating all hangings, will occur when the following condition is met:

$$H < 3L_e, \quad (20)$$

where:

$L_e$  – equivalent span of the unsupported mined-out space (caving zone).

After the completion of secondary extraction of one panel, the equivalent span of the caving zone was  $L_e = 70$  m. At a depth of  $H = 550$  m, Criterion (20) is unsatisfied. Consequently, after one panel is mined out, the caving zone forms an arch, while the overlying strata remain hanging on the barrier pillars, concentrating significant support pressure on them. Extraction of such heavily loaded barrier pillars is therefore complicated.

Criterion (20) is satisfied only after extracting three panels and the two barrier pillars between them. In this case, the span of the caved zone reaches 270 m, and the condition  $H < 3 \cdot L_e$  is fulfilled ( $550 < 810$ ). Thus, secondary extraction of the first two barrier pillars requires additional measures to unload them from support pressure.

Numerical modeling was carried out using the Examine 2D software (RocScience, Canada) to determine the composition of such measures. The input parameters were as follows: ground surface elevation – 360 m; unit weight of rocks –  $2.7 \text{ t/m}^3$ ; lateral pressure coefficients: in the plane of section – 2, perpendicular to the section – 1.2; deformation modulus of the rock mass – 4700 MPa; Poisson's ratio – 0.2; tensile strength of the rock mass – 2 MPa; cohesion – 8.7 MPa; internal friction angle –  $35^\circ$ ; compressive strength of the rock mass – 33 MPa.

Figure 20 presents the calculated stability of the rock mass after secondary extraction of a single panel with a mining height  $h = 7$  m and width  $L = 70$  m at a depth  $H = 550$  m (floor elevation -210 m).

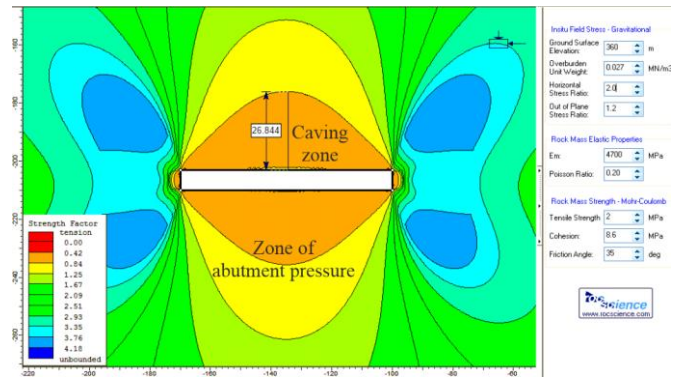


Figure 20. Stability assessment of the rock mass after the extraction of a single panel

The caving zone, where the Coulomb-Mohr strength factor is less than 1, is highlighted in orange. Its height above the mined-out space is  $h_0 = 27$  m. The ratio of caving zone height to its span is  $h_0/L = 0.4$ .

For the conditions of the Zhezkazgan deposit, this ratio is lower and equals  $h_0/L = 0.3$ . Thus, under the conditions of the Zhomart mine, due to lower rock strength and reduced horizontal stress levels, the arch formed during caving is steeper than at the Zhezkazgan mines.

It should be noted that the failure zone develops above the mined-out space and beneath it. On the sides of the mined-out area, rather extensive zones of volumetric compression are formed due to support pressure and horizontal confinement, with safety factors of 3 or higher.

A similar pattern is observed in the modeling of multiple-panel extraction. Figure 21 presents the calculated stability of the rock mass after extracting two panels with a 30 m barrier pillar left between them. Within the barrier pillar itself and in the zones above and below it, an area of volumetric compression with a high safety factor is formed.

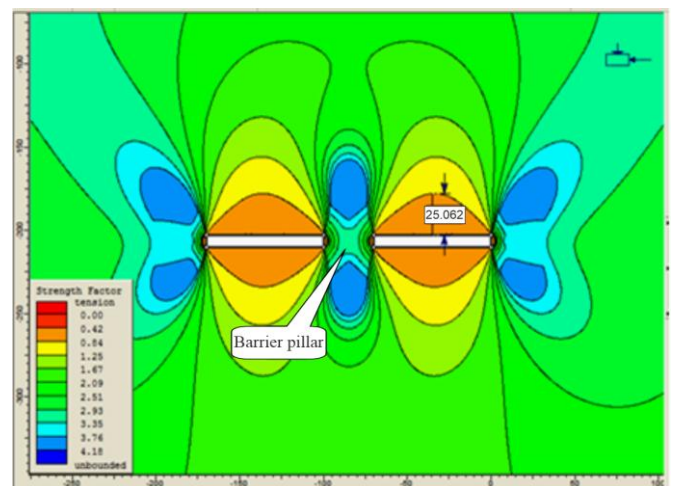


Figure 21. Stability assessment of the rock mass after the extraction of two panels with one barrier pillar left between them

Their geometric parameters determine the formation of volumetric compression zones in the barrier pillars: the pillar width is four times its height, which practically eliminates the possibility of significant displacements. Figure 22 clearly shows that displacements within the barrier pillars themselves are minimal. As a result, they function as dividing elements, localizing and separating individual caving zones.

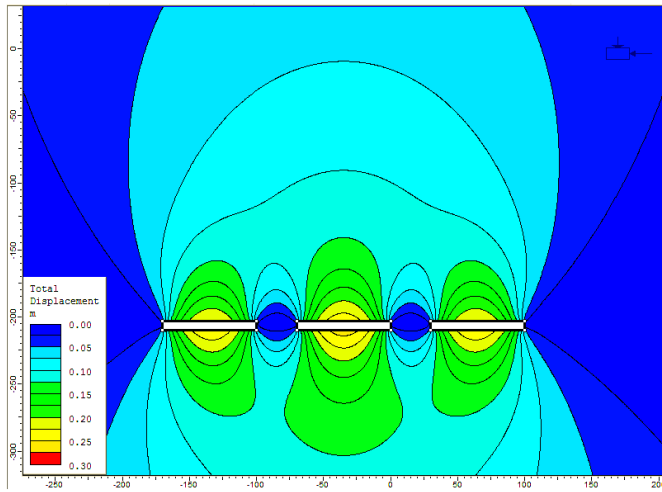


Figure 22. Rock mass displacements after the extraction of three panels with a barrier pillar between them

The development of drill drifts within them would be required to enable the subsequent extraction of barrier pillars. However, the probability of maintaining their stability is extremely low due to the high stress levels. Figure 23 presents an assessment of the stability of a drill drift with a 4×4 m cross-section driven along the axis of a barrier pillar. The calculation shows that under such conditions, the drift undergoes failure already at the initial stages of operation, which makes this method technologically unfeasible without additional rock mass unloading measures.

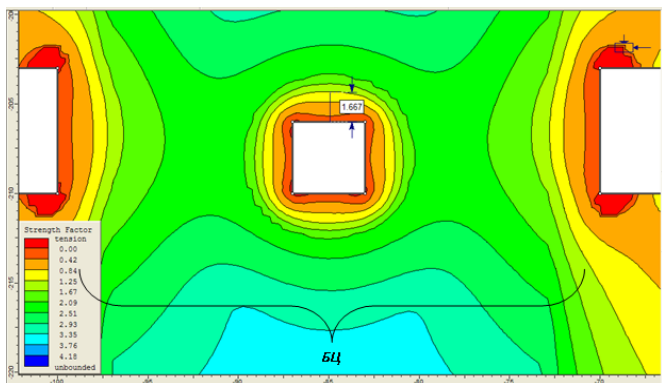


Figure 23. Failure of a drill drift driven along the axis of a barrier pillar

When a drill drift is driven through a barrier pillar, rock mass failure occurs to a depth of up to 1.7 m in all directions: roof, ribs, and floor of the excavation. Given the brittle nature of the ore and the high level of in-situ stresses, these failures are accompanied by manifestations of rock bursts. Using conventional support systems, such as rock bolts and shotcrete, does not prevent such failures. In addition, the side portions of the pillar are crushed to a depth of up to 2 m.

Even after the extraction of a single barrier pillar, the stress-strain state of the rock mass remains unfavorable. As shown in Figure 24, the caving arch above the mined-out pillar rises to a height of up to 64 m, while the ratio of the caving zone height to the span of underworked space remains constant ( $h_0/L = 0.4$ ). A zone of volumetric compression develops in the adjacent barrier pillar due to the combined effect of support pressure and horizontal tectonic stresses.

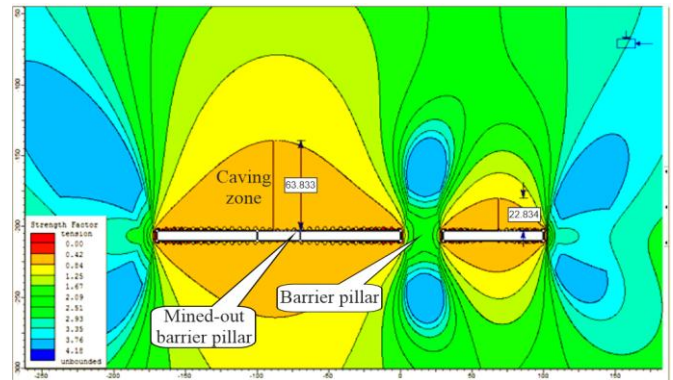


Figure 24. Stability of the rock mass after the extraction of three panels and one barrier pillar

To unload barrier pillars from excessive support pressure, it is necessary to ensure their indentation into the roof and floor rocks of the ore body. This process is analogous to pressing a rigid punch into a brittle medium: a triangular compaction core is formed beneath the punch (or conical in the case of a circular punch), beyond which a spalling funnel develops. The same effect underlies the drilling of blast holes and boreholes using carbide-tipped core bits.

In the case of barrier pillar indentation into the surrounding rocks, the subsidence of the overburden occurs, which reduces the load on the pillar to the level of the natural pressure  $\gamma H$ . The scheme of the sliding system, including the major fractures that form at the limiting state during the subsidence of the overlying strata, is shown in Figure 25.

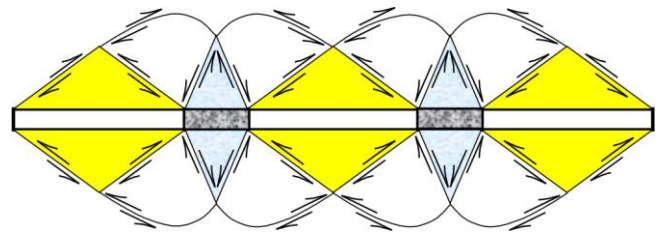


Figure 25. Slip-line system formed during the subsidence of overburden onto barrier pillars

The stresses at which pillar indentation into the foundation rocks occurs are determined according to the formula of G.L. Fisenko:

$$\sigma_1 = \sigma_m \left( 1 + \operatorname{tg}^2 \left( \frac{\pi}{4} + \frac{\varphi}{2} \right) \right). \quad (21)$$

For the conditions of the Zhomart mine, the calculations showed that the stresses required for barrier pillar indentation into the surrounding rocks exceed 150 MPa. The average acting stresses in the pillars amount to about 49 MPa, which is insufficient for the spontaneous development of the subsidence process. Therefore, it must be artificially initiated.

A practical method is the use of camouflet blasting of charges in boreholes drilled above the barrier pillars. As a result of localized blasting, zones of fracturing and loosening are formed in the roof, which leads to the subsidence of the overburden onto the pillars and reduces their loading to the level of natural pressure. The arrangement of the process is illustrated in Figure 26.

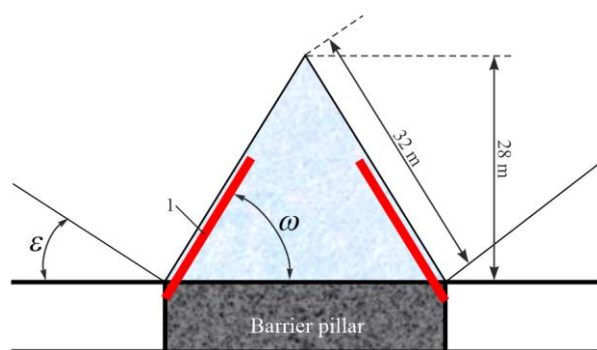


Figure 26. Subsidence of the overburden onto barrier pillars using camouflet blasting of boreholes in the roof

Boreholes for camouflet blasting should be drilled from the upper corner of the barrier pillar into the roof at an angle corresponding to the slip line. According to limit equilibrium theory, the inclination angles of slip surfaces are determined by Equations (22) and (23):

$$\omega = \frac{\pi}{4} + \frac{\varphi}{2}; \quad (22)$$

$$\varepsilon = \frac{\pi}{4} - \frac{\varphi}{2}. \quad (23)$$

For  $\varphi = 35^\circ$ , the inclination angles of the slip lines are  $\omega = 62^\circ$  and  $\varepsilon = 28^\circ$ . Thus, the optimal drilling angle for boreholes is  $62^\circ$ , as shown in Figure 26. Boreholes should be collared as close as possible to the roof.

For a barrier pillar width of  $A = 30$  m, the height of the compaction core above and below the pillar is 28 m, while the length of slip lines inclined at angle  $\omega$  is 32 m. In this case, the maximum borehole dimensions are limited by the drilling equipment available. If a row of boreholes is drilled at 1 m spacing and 20 m depth, camouflet blasting will break the bonding along two-thirds of the slip line length. This action will induce subsidence of the overburden onto the barrier pillars, reduce their support pressure, and create favorable conditions for subsequent drift development through the pillar.

Comprehensive studies conducted under the conditions of the Zhomart mine have shown that the strength characteristics of the ore mass and the host rocks are significantly lower than those at the Zhezkazgan deposit, which had previously been considered a benchmark analogue. This factor necessitates the adjustment of room-and-pillar system parameters and the improvement of applied ground support technologies [56]–[58].

The analysis demonstrated that the optimal system parameters should include a panel span of about 70 m, an extraction room width of 7 m, and an inter-room pillar grid of  $16 \times 16$  m with pillar diameters of 9 m and cross-sectional areas of about  $64 \text{ m}^2$ . The necessity of employing warning pillars with an area of  $18\text{--}20 \text{ m}^2$  has been experimentally confirmed; these pillars operate in an overstressed deformation regime and provide controlled caving of the immediate roof. The calculated width of barrier pillars required to ensure an adequate safety factor is 30 m.

Field observations and instrumental measurements revealed significant defects in the steel-polymer bolt supports: rod failures along the threaded section and breakages of bearing plates. Such defects initiate a chain reaction of failures, leading to large-scale roof collapses. As a constructive alternative, the use of rope-thread bolts of the A20V type is justifi-

fied, as they provide higher load-bearing capacity and better adaptation to the geomechanical conditions of the deposit.

Numerical modeling conducted using the CPS 2005, Pillars 3, and Examine 2D software confirmed the effectiveness of the proposed parameters. It was established that the safety factor of inter-room pillars reaches 1.9–2.0, while the stability of barrier pillars remains at the level of  $n \approx 2.1$ . In addition, the feasibility of camouflet blasting of boreholes above barrier pillars has been demonstrated to initiate overburden subsidence and reduce the concentration of support pressure.

Comparison with international studies reveals similar trends. For example, Walton et al. [59], based on data from deep mines in the United States, established that the safety factor of pillars under high jointing conditions should not fall below 2.0, coinciding with the Zhomart deposit's modeling results. The authors also noted that using narrow extraction rooms and adjusting pillar spacing can significantly reduce the scale of roof collapses, which supports the relevance of the proposed parameters.

Similarly, Guo et al. [60], studying the operation of copper mines in China, showed that the long-term stability of barrier pillars directly depends on their width and the regularity of their grid arrangement. In particular, it was established that the probability of progressive collapses increases significantly at widths below 25–30 m. The parameters obtained for Zhaman-Aibat fully correspond to these findings and demonstrate the universality of approaches to ensuring the stability of room-and-pillar systems.

Thus, the conducted research has made it possible to develop scientifically grounded recommendations to improve the mining system's stability, reduce ore losses, and minimize geotechnical risks. The obtained results have high practical significance and can be applied in the design and operation of mines that develop deposits of a similar geological-structural type.

Based on analytical calculations, field observations, and numerical modeling, the following rational parameters of the room-and-pillar system are proposed for industrial trials: spacing of barrier pillars – 100 m, with a calculated width of 30 m; panel span (clear width) – not more than 70 m; inter-room pillars arranged on a  $16 \times 16$  m grid with a diameter of 9 m and a cross-sectional area of  $64 \text{ m}^2$ ; extraction room width – 7 m, with the optimal number of rooms per panel being five; for temporary support of the immediate roof, it is recommended to leave warning pillars with an area of  $18\text{--}20 \text{ m}^2$ .

In addition, during the blasting of inter-room pillars adjacent to barrier pillars, it is advisable to carry out camouflet blasting of boreholes drilled above the barrier pillars. This technological measure ensures controlled subsidence of the overburden, unloading of barrier pillars from excessive support pressure, and improved overall stability of the rock mass during stoping operations.

## 5. Conclusions

Comprehensive studies conducted under the conditions of the Zhomart mine confirmed that the physico-mechanical properties of the ore body and host rocks are significantly lower than those of the Zhezkazgan deposit, which has traditionally been considered the reference analogue. This necessitated the adjustment of the parameters of the room-and-pillar mining system.



The optimal system parameters include: a panel span (clear width) of about 70 m, an extraction room width of 7 m, a grid of inter-room pillars 16×16 m with a diameter of 9 m and a cross-sectional area of about 64 m<sup>2</sup>. These parameters ensure a safety factor for inter-room pillars in the range of 1.9-2.0.

The necessity of applying warning pillars with an 18-20 m<sup>2</sup> area has been experimentally confirmed. They operate in an ultimate deformation regime, allowing temporary and controlled support of the immediate roof with a thickness of up to 10 m, preventing sudden collapses and ensuring managed subsidence of the overburden.

The calculated width of barrier pillars should be 30 m. This value guarantees a safety factor of about 2.1, corresponding to accepted reliability requirements in practice and ensuring the localization of caving zones.

Field observations and testing revealed structural defects in steel-polymer bolts with metric threads (rod breakages and failures of bearing plates). An alternative solution, bolts with a rope thread of type A20B, has been proposed, providing higher load-bearing capacity and better adaptation to the geomechanical conditions of Zhomart.

The proposed technical solutions improve mining safety, reduce ore losses in pillars, ensure controlled subsidence of the overburden, and minimize geotechnical risks in exploiting deposits of a similar geological-structural type.

#### Author contributions

Conceptualization: BA, IA; Data curation: BU; Formal analysis: AB, ArK; Funding acquisition: IA; Investigation: BU, ZS; Methodology: BU, AiK; Project administration: BA, ArK; Resources: AB; Software: BU, IA; Supervision: AiK; Validation: BA, IA; Visualization: BU, ArK; Writing – original draft: AB; Writing – review & editing: BU, ZS, AiK. All authors have read and agreed to the published version of the manuscript.

#### Funding

This research received no external funding.

#### Conflicts of interest

The authors declare no conflict of interest.

#### Data availability statement

The original contributions presented in the study are included in the article, further inquiries can be directed to the corresponding author.

#### References

- [1] Kunarbekova, M., Yeszhan, Y., Zharylkan, S., Alipuly, M., Zhan-tikeev, U., Beisebayeva, A., Kudaibergenov, A., Rysbekov, K., Toktarbay, Z., & Azat, S. (2024). The state of the art of the mining and metallurgical industry in Kazakhstan and future perspectives: A systematic review. *ES Materials & Manufacturing*, 25, 1219. <https://doi.org/10.30919/esmm1219>
- [2] Bekbassarov, S., Soltabayeva, S., Daurenbekova, A., & Ormanbekova, A. (2015). "Green" economy in mining. *New Developments in Mining Engineering 2015: Theoretical and Practical Solutions of Mineral Resources Mining*, 431-434. <https://doi.org/10.1201/b19901-75>
- [3] Pavlychenko, A.V., Ihnatov, A.O., Koroviaka, Y.A., Ratov, B.T., & Zakenov, S.T. (2022). Problematics of the issues concerning development of energy-saving and environmentally efficient technologies of well construction. *IOP Conference Series: Earth and Environmental Science*, 1049(1), 012031. <https://doi.org/10.1088/1755-1315/1049/1/012031>
- [4] Baibatyrova, B., Tileuberdi, A., Begentayev, M., Kuldeyev, E., Nyrlybayev, R., Altybayev, Z., Sarsenbayev, B., Abduova, A., & Sauganova, G. (2024). Improving the methods of solid domestic waste disposal to reduce its human impact on the environment. *Sustainability*, 16(24), 11071. <https://doi.org/10.3390/su162411071>
- [5] Hapich, H., Andrieiev, V., Kovalenko, V., Hrytsan, Y., & Pavlychenko, A. (2022). Study of fragmentation impact of small riverbeds by artificial waters on the quality of water resources. *Naukovyi Visnyk Natsionalnoho Hirnychoho Universytetu*, 3, 185-189. <https://doi.org/10.33271/nvngu/2022-3/185>
- [6] Kholodenko, T., Ustimenko, Y., Pidkamenna, L., & Pavlychenko, A. (2014). Ecological safety of emulsion explosives use at mining enterprises. *Progressive Technologies of Coal, Coalbed Methane, and Ores Mining*, 255-260. <https://doi.org/10.1201/b17547>
- [7] Matayev, A.K., Kainazarova, A.S., Arystan, I.D., Abeuov, Ye., Kainazarov, A.S., Baizbayev, M.B., Demin, V.F., & Sultanov, M.G. (2021). Research into rock mass geomechanical situation in the zone of stope operations influence at the 10<sup>th</sup> Anniversary of Kazakhstan's Independence mine. *Mining of Mineral Deposits*, 15(1), 1-10. <https://doi.org/10.33271/mining15.01.042>
- [8] Nurpeisova, M.B., Salkynov, A.T., Soltabayeva, S.T., & Miletchenko, N.A. (2024). Patterns of development of geomechanical processes during hybrid open pit/underground mineral mining. *Eurasian Mining*, 41(1), 7-11. <https://doi.org/10.17580/em.2024.01.02>
- [9] Volkov, A.P., Buktukov, N.S., & Kuanyshbauly, S. (2022). Safe and effective methods for mining thin tilt and steeply dipping deposits with ore drawing via mud flow. *Gornyi Zhurnal*, 4, 86-91. <https://doi.org/10.17580/gzh.2022.04.13>
- [10] Sailygarayeva, M., Nurlan, A., Rysbekov, K., Soltabayeva, S., Amralinova, B., & Baygurin, Z. (2023). Predicting of vertical displacements of structures of engineering buildings and facilities. *Naukovyi Visnyk Natsionalnoho Hirnychoho Universytetu*, 2, 77-83. <https://doi.org/10.33271/nvngu/2023-2/077>
- [11] Daineko, Y.A., Duzbayev, N.T., Kozhaly, K.B., Ipalakova, M.T., Bekaulova, Z.M., Nalgozhina, N.Z., & Sharshova, R.N. (2020). The use of new technologies in the organization of the educational process. *Intelligent Computing: Proceedings of the 2020 Computing Conference*, 3, 622-627. [https://doi.org/10.1007/978-3-030-52243-8\\_46](https://doi.org/10.1007/978-3-030-52243-8_46)
- [12] Moldabayeva, G.Z., Turdiyev, M.F., Suleimenova, R.T., Buktukov, N.S., Efendiyev, G.M., Kodanova, S.K., & Tuzelbayeva, S.R. (2025). Application of the integrated well-surface facility production system for selecting the optimal operating mode of equipment. *Complex Use of Mineral Resources*, 335(4), 96-109. <https://doi.org/10.31643/2025/6445.44>
- [13] Rudenko, O., Galkina, D., Sadenova, M., Beisekenov, N., Kuliz, M., & Begentayev, M. (2024). Modelling the properties of aerated concrete on the basis of raw materials and ash-and-slag wastes using machine learning paradigm. *Frontiers in Materials*, 11, 1481871. <https://doi.org/10.3389/fmats.2024.1481871>
- [14] Muratova, S., Pashchenko, O., Khomenko, V., & Zhailiev, A. (2025). Application of machine learning for wellbore stability assessment. *Engineering for Rural Development*, 24, 505-511. <https://doi.org/10.22616/ERDev.2025.24.TF109>
- [15] Kondratyev, S.I., Baskanbayeva, D., Yelemessov, K., Khekert, E.V., Privalov, V.E., Sarsenbayev, Y., & Turkin, V. A. (2024). Control of hydrogen leaks from storage tanks and fuel supply systems to mining transport infrastructure facilities. *International Journal of Hydrogen Energy*, 95, 212-216. <https://doi.org/10.1016/j.ijhydene.2024.11.182>
- [16] Yelemessov, K.K., Baskanbayeva, D.D., Sabirova, L.B., & Akhmetova, S.D. (2023). Justification of an acceptable modern energy-efficient method of obtaining sodium silicate for production in Kazakhstan. *IOP Conference Series: Earth and Environmental Science*, 1254(1), 012002. <https://doi.org/10.1088/1755-1315/1254/1/012002>
- [17] Buktukov, N., Gumennikov, Y., & Moldabayeva, G. (2024). Solutions to the problems of transition to green energy in Kazakhstan. *World-Systems Evolution and Global Futures*, 113-133. [https://doi.org/10.1007/978-3-031-67583-6\\_6](https://doi.org/10.1007/978-3-031-67583-6_6)
- [18] Kezembayeva, G., Rysbekov, K., Dyussenova, Z., Zhumagulov, A., Umbetaly, S., Barmenshinova, M., Yerkezhan, B., & Zhakypbek, Y. (2025). Public health risk assessment of quantitative emission from a molybdenum production plant: Case study of Kazakhstan. *Engineered Science*, 34, 1454. <https://doi.org/10.30919/es1454>
- [19] Turegeldinova, A., Amralinova, B., Fodor, M.M., Rakhmetullina, S., Konurbayeva, Z., & Kiizbayeva, Z. (2024). STEM and the creative and cultural industries: the factors keeping engineers from careers in the CCLs. *Frontiers in Communication*, 9, 1507039. <https://doi.org/10.3389/fcomm.2024.1507039>
- [20] Zhakypbek, Y., Belkozhaev, A. M., Kerimkulova, A., Kossalbayev, B.D., Murat, T., Tursbekov, S., & Allakhverdiev, S.I. (2025). MicroRNAs in

- plant genetic regulation of drought tolerance and their function in enhancing stress adaptation. *Plants*, 14(3), 410. <https://doi.org/10.3390/plants14030410>
- [21] Konysbayeva, A., Yessimsitova, Z., Toktar, M., Mutushev, A., Zhakypbek, Y., Tursbekov, S., Tursbekova, G., Kozhayev, Z., Kozhamzharova, A., Mombekov, S., & Raheem, S. (2025). Result of reclamation of man-made dumps from phosphorite deposits in the semi-desert zone of Kazakhstan. *PloS ONE*, 20(2), e0317500. <https://doi.org/10.1371/journal.pone.0317500>
- [22] Baibatsha, A.B. (2002). *Geologiya mestorozhdeniy poleznykh iskopaemykh*. Almaty, Kazakhstan: Kazakh National Technical University. Available at: <https://www.geokniga.org/bookfiles/geokniga-baybatshageologiyampi.pdf>
- [23] Amralinova, B.B., Frolova, O.V., Mataibaeva, I.E., Agaliyeva, B.B., & Khromykh, S.V. (2021). Mineralization of rare metals in the lakes of East Kazakhstan. *Naukovyi Visnyk Natsionalnoho Hirnychoho Universytetu*, 5, 16-21. <https://doi.org/10.33271/nvngu/2021-5/016>
- [24] Umarbekova, Z.T., Zholtayev, G.Z., Zholtayev, G.Z., Amralinova, B.B., & Mataibaeva, I.E. (2020). Silver halides in the hypergene zone of the Arkharly gold deposit as indicators of their formation in dry and hot climate (Dzungar Alatau, Kazakhstan). *International Journal of Engineering Research and Technology*, 13(1), 181-190. <https://doi.org/10.37624/ijert/13.1.2020.181-190>
- [25] Dyachkov, B.A., Aitbayeva, S.S., Mizemaya, M.A., Amralinova, B.B., & Bissatova, A.E. (2020). New data on non-traditional types of East Kazakhstan rare metal ore. *Naukovyi Visnyk Natsionalnoho Hirnychoho Universytetu*, 4, 11-16. <https://doi.org/10.33271/nvngu/2020-4/011>
- [26] Dyachkov, B.A., Amralinova, B.B., Mataybaeva, I.E., Dolgoplova, A.V., Mizerny, A.I., & Mirosnikova, A. P. (2017). Laws of formation and criteria for predicting nickel content in weathering crusts of east Kazakhstan. *Journal of the Geological Society of India*, 89(5), 605-609. <https://doi.org/10.1007/s12594-017-0650-7>
- [27] Ahmadi, H., Hussaini, M.R., Yousufi, A., Bekbotayeva, A., Baisalova, A., Amralinova, B., Mataibaeva, I., Rahmani, A.B., Pekkan, E., & Sahak, N. (2023). Geospatial insights into ophiolitic complexes in the Cimmerian realm of the Afghan central block (Middle Afghanistan). *Minerals*, 13(11), 1453. <https://doi.org/10.3390/min13111453>
- [28] Efendiyeu, G.M., Moldabayeva, G.Z., Buktukov, N.S., & Kuliyeu, M.Y. (2024). Comprehensive cementing quality assessment and risk management system. *SOCAR Proceedings*, 4, 42-47. <https://doi.org/10.5510/OGP20240401015>
- [29] Myrzakulov, M.K., Jumankulova, S.K., Barmenshinova, M.B., Martyshev, N.V., Skeebe, V.Y., Kondratiev, V.V., & Karlina, A.I. (2024). Thermodynamic and technological studies of the electric smelting of Satpaevsk ilmenite concentrates. *Metals*, 14(11), 1211. <https://doi.org/10.3390/met14111211>
- [30] Myrzakulov, M.K., Dzhumankulova, S.K., Yelemessov, K.K., Barmenshinova, M.B., Martyshev, N.V., Skeebe, V.Y., Kondratiev, V.V., & Karlina, A.I. (2024). Analysis of the effect of fluxing additives in the production of titanium slags in laboratory conditions. *Metals*, 14(12), 1320. <https://doi.org/10.3390/met14121320>
- [31] Zhagifarov, A.M., Akhmetov, D.A., Suleyev, D.K., Zhumadilova, Z.O., Begentayev, M.M., & Pukhareno, Y.V. (2024). Investigation of hydro-physical properties and corrosion resistance of modified self-compacting concretes. *Materials*, 17(11), 2605. <https://doi.org/10.3390/ma17112605>
- [32] Imanskipova, B.B., Baygurin, Z.D., Soltabaeva, S.T., Milev, I., & Miletchenko, I.V. (2014). Causes of strain of buildings and structures in areas of abnormal stress and surveillance terrestrial laser scanners. *Life Science Journal*, 11(9s), 165-170.
- [33] Akhmetkanov, D.K. (2023). New variants for wide orebodies high-capacity mining systems with controlled and continuous in-line stoping. *News of the National Academy of Sciences of the Republic of Kazakhstan, Series of Geology and Technical Sciences*, 3(459), 6-21. <https://doi.org/10.32014/2023.2518-170X.295>
- [34] Pashchenko, O.A., Khomenko, V.L., Ratov, B.T., Koroviaka, Ye.A., & Rastsvietaiev, V.O. (2024). Comprehensive approach to calculating operational parameters in hydraulic fracturing. *IOP Conference Series: Earth and Environmental Science*, 1415(1), 012080. <https://doi.org/10.1088/1755-1315/1415/1/012080>
- [35] Golik, V.I., Klyuev, R.V., Martyshev, N.V., Zyukin, D.A., & Karlina, A.I. (2024). Determination of safe spans of mine workings based on the bearing capacity of rocks in deposit development. *Mining Industry*, 55, 59-63.
- [36] Yu, Y., Chen, S., Deng, K.Z., & Fan, H.D. (2017). Long-term stability evaluation and pillar design criterion for room-and-pillar mines. *Energies*, 10(10), 1644. <https://doi.org/10.3390/en10101644>
- [37] Stupnik, M., Kalinichenko, V., & Pismennyi, S. (2013). Pillars sizing at magnetite quartzites room-work. *Annual Scientific-Technical Collec-*
- tion – Mining of Mineral Deposits* 2013, 11-15. <https://doi.org/10.1201/b16354-3>
- [38] García-Gonzalo, E., Fernández-Muñiz, Z., García Nieto, P.J., Bernardo Sánchez, A., & Menéndez Fernández, M. (2016). Hard-rock stability analysis for span design in entry-type excavations with learning classifiers. *Materials*, 9(7), 531. <https://doi.org/10.3390/ma9070531>
- [39] Yu, Y., Zhang, Q., Yang, X., Wang, Y., & Li, Z. (2017). Long-term stability evaluation and pillar design criterion. *Energies*, 10(10), 1644. <https://doi.org/10.3390/en10101644>
- [40] Nazarov, L.A., Nazarova, L.A., & Freidin, A.M. (2006). Estimating the long-term pillar safety for room-and-pillar ore mining. *Journal of Mining Science*, 42(5), 530-539. <https://doi.org/10.1007/s10913-006-0096-6>
- [41] Walton, G., Esterhuizen, G.S., & Tulu, I.B. (2021). Improved empirical hard rock pillar strength predictions using unconfined compressive strength as a proxy for brittleness. *International Journal of Rock Mechanics and Mining Sciences*, 148, 104934. <https://doi.org/10.1016/j.ijrmms.2021.104934>
- [42] Moffat, R., Rodriguez, R., & Varas, F. (2021). Rock pillar design using a masonry equivalent numerical model. *Energies*, 14(4), 890. <https://doi.org/10.3390/en14040890>
- [43] Toderas, M., Răileanu, P., Şeclăman, M., & Ilie, C. (2024). Stability analysis of the exploitation system with room and pillars. *Applied Sciences*, 14(5), 1827. <https://doi.org/10.3390/app14051827>
- [44] Liu, H., Li, C., Li, J., & Yang, W. (2022). Study on stability of underlying room and pillar old goaf. *Frontiers in Earth Science*, 10, 1071250. <https://doi.org/10.3389/feart.2022.1071250>
- [45] Guo, J., Xu, X., Zhang, H., & Zhou, Y. (2022). Research on factors affecting mine wall stability in isolated pillar mining in deep mines. *Minerals*, 12(5), 623. <https://doi.org/10.3390/min12050623>
- [46] Li, N., Zare, M., Yi, C., & Jimenez, R. (2022). Stability risk assessment of underground rock pillars using logistic model trees. *International Journal of Environmental Research and Public Health*, 19(4), 2136. <https://doi.org/10.3390/ijerph19042136>
- [47] Alejano, L.R., Arzúa, J., Castro-Filgueira, U., & Malan, F. (2017). Strapping of pillars with cables to enhance pillar stability. *Journal of the Southern African Institute of Mining and Metallurgy*, 117(6), 527-540. <https://doi.org/10.17159/2411-9717/2017/v117n6a7>
- [48] Demin, V., Kalinin, A., Baimuldin, M., Tomilov, A., Smagulova, A., Mutovina, N., Shokarev, D., Aliev, S., Akpanbayeva, A., & Demina, T. (2024). Developing a technology for driving mine workings with combined support and friction anchors in ore mines. *Applied Sciences*, 14(22), 10344. <https://doi.org/10.3390/app142210344>
- [49] Arystan, I.D., Nemova, N.A., Baizbaev, M.B., & Mataev, A.K. (2021). Efficiency of modified concrete in lining in underground structures. *IOP Conference Series. Earth and Environmental Science*, 773(1), 012063. <https://doi.org/10.1088/1755-1315/773/1/012063>
- [50] Arystan, I.D., Baizbaev, M.B., Mataev, A.K., Abdieva, L.M., & Bogzhanova, Z.K. (2020). Selection and justification of technology for fixing preparatory workings in unstable massifs on the example of the mine “10 years of Independence of Kazakhstan. *Ugol*, 6, 10-14. <https://doi.org/10.18796/0041-5790-2020-6-10-14>
- [51] Sultanov, M.G., Mataev, A.K., Kaumetova, D.S., Abdrashev, R.M., Kuantay, A.S., & Orynbayev, B.M. (2020). Development of the choice of types of support parameters and technologies for their construction at the Voskhod field. *Ugol*, 10, 17-21. <https://doi.org/10.18796/0041-5790-2020-10-17-21>
- [52] Istekova, S., Makarov, A., Tolybaeva, D., Sirazhev, A., & Togizov, K. (2024). Determining the boundaries of overlying strata collapse above mined-out panels of Zhomart mine using seismic data. *Geosciences*, 14(11), 310. <https://doi.org/10.3390/geosciences14110310>
- [53] Rysbekov, K.B., Bitimbayev, M.Z., Akhmetkanov, D.K., & Miletchenko, N.A. (2022). Improvement and systematization of principles and process flows in mineral mining in the Republic of Kazakhstan. *Eurasian Mining*, 1, 41-45. <https://doi.org/10.17580/em.2022.01.08>
- [54] Majeed, Y., Abbas, N., & Emad, M. Z. (2023). Stability evaluation of room-and-pillar rock salt mines by using a flat jack technique – A case study. *Journal of the Southern African Institute of Mining and Metallurgy*, 123(6), 287-298. <https://doi.org/10.17159/2411-9717/1872/2023>
- [55] Aitaliyev, S.M., & Takishov, A.A. (2000). Control of arch formation in the room-and-pillar system of mining. Part I. Stress-strain state of the rock mass. *Journal of Mining Science*, 36(2), 97-105. <https://doi.org/10.1007/BF02551788>
- [56] Nurpeisova, M.B., Bitimbayev, M.Z., Rysbekov, K.B., & Bekbasarov, S.S. (2021). Forecast changes in the geodynamic regime of geological environment during large-scale subsoil development. *Naukovyi Visnyk Natsionalnoho Hirnychoho Universytetu*, 6, 5-10. <https://doi.org/10.33271/nvngu/2021-6/005>

- [57] Lozynskyi, V., Yussupov, K., Rysbekov, K., Rustemov, S., & Bazaluk, O. (2024). Using sectional blasting to improve the efficiency of making cut cavities in underground mine workings. *Frontiers in Earth Science*, 12, 1366901. <https://doi.org/10.3389/feart.2024.1366901>
- [58] Rysbekov, K.B., Kyrgyzbayeva, D.M., Miletchenko, N.A., & Kuandykov, T.A. (2024). Integrated monitoring of the area of Zhilandy deposits. *Eurasian Mining*, 41(1), 3-6. <https://doi.org/10.17580/em.2024.01.01>
- [59] Bazaluk, O., Petlovanyi, M., Zubko, S., Lozynskyi, V., & Sai, K. (2021). Instability assessment of hanging wall rocks during underground mining of iron ores. *Minerals*, 11(8), 858. <https://doi.org/10.3390/min11080858>
- [60] Guo, J., Xu, X., Zhang, H., & Zhou, Y. (2022). Research on factors affecting mine wall stability in isolated pillar mining in deep mines. *Minerals*, 12(5), 623. <https://doi.org/10.3390/min12050623>

### Комплексна геомеханічна оцінка стійкості ціликів і покрівлі при повторному відпрацюванні камерно-стовповою системою

Б. Уахітова, Б. Алматова, А. Балгинова, Ж. Шилмагамбетова, І. Аристан, А. Куантаєва, А. Карабатирова

**Мета.** Дослідження спрямоване на обґрунтування раціональних параметрів камерно-стовпової системи розробки мідистих пісковиків родовища Жаман-Айбат (рудник Жомарт) з урахуванням геомеханічних особливостей масиву.

**Методика.** У роботі використано аналітичні розрахунки за методиками Шевякова, Церна та Чернікова, числове моделювання (програми комплексу CPS 2005, Pillars 3, Examine 2D), а також дані натурних спостережень і дослідно-промислових випробувань. Розрахунок стійкості міжкамерних і бар'єрних ціликів виконано методом ітерацій з урахуванням коефіцієнта форми, навантаження та довготривалої міцності. Експериментально перевірено ефективність сигнальних ціликів і різних типів анкерного кріплення.

**Результати.** Встановлено, що оптимальні параметри системи включають: проліт панелі у світлі близько 70 м, ширину очисних камер 7 м, сітку розташування міжкамерних ціликів 16×16 м при діаметрі 9 м (площа 64 м<sup>2</sup>). Експериментально обґрунтовано необхідність залишення сигнальних ціликів площею 18-20 м<sup>2</sup>, що працюють у режимі граничного деформування. Розрахункова ширина бар'єрних ціликів становить 30 м, при цьому коефіцієнт запасу міцності досягає  $n \approx 2.1$ . Виявлено конструктивні недоліки сталеполімерних анкерів із метричною різьбою, що ініціюють ланцюгову реакцію руйнувань; запропоновано використовувати анкери з канатною різьбою типу А20В. Числове моделювання показало, що застосування камуфлетного підривання свердловин над бар'єрними ціликами сприяє розвантаженню масиву та зниженню концентрації опорного тиску.

**Наукова новизна.** Вперше для умов рудника Жомарт проведено комплексну оцінку стійкості міжкамерних, сигнальних і бар'єрних ціликів із використанням даних зворотних розрахунків та натурних спостережень. Встановлено кількісну залежність параметрів сигнальних ціликів у режимі граничного деформування й обґрунтовано необхідність їх обов'язкового застосування. Обґрунтовано ефективність використання камуфлетного підривання для контрольованої посадки надлежачої товщі.

**Практична значимість.** Розроблені рекомендації дозволяють знизити втрати руди в ціликах, підвищити стійкість системи розробки та мінімізувати гірничий ризик. Отримані результати можуть бути використані при проєктуванні та експлуатації рудників аналогічного геолого-структурного типу.

**Ключові слова:** Жаман-Айбат, рудник Жомарт, камерно-стовпова система, міжкамерні цілики, бар'єрні цілики, анкерне кріплення, стійкість масиву

### Publisher's note

All claims expressed in this manuscript are solely those of the authors and do not necessarily represent those of their affiliated organizations, or those of the publisher, the editors and the reviewers.